The Smaller (SALI) and the Generalized (GALI) Alignment Indices: Efficient methods of chaos detection

Haris Skokos

Department of Mathematics and Applied Mathematics
University of Cape Town, Cape Town, South Africa

E-mail: haris.skokos@uct.ac.za
URL: http://www.mth.uct.ac.za/~hskokos/

Work in collaboration with
Tassos Bountis, Chris Antonopoulos, Thanos Manos

Outline

- **Hamiltonian systems – Symplectic maps**
  - ✓ **Variational equations**
  - ✓ **Poincaré Surface of Section**
  - ✓ **Lyapunov exponents**

- **Smaller ALignment Index – SALI**
  - ✓ **Definition**
  - ✓ **Behavior for chaotic and regular motion**
  - ✓ **Applications**

- **Generalized ALignment Index – GALI**
  - ✓ **Definition - Relation to SALI**
  - ✓ **Behavior for chaotic and regular motion**
  - ✓ **Applications**
  - ✓ **Global dynamics**
  - ✓ **Time-dependent Hamiltonians**

- **Conclusions**

Autonomous Hamiltonian systems

Consider an N degree of freedom autonomous Hamiltonian system having a Hamiltonian function of the form:

$$H(\overbrace{q_1,q_2,\ldots,q_N}^{\text{positions}}, \overbrace{p_1,p_2,\ldots,p_N}^{\text{momenta}})$$

The time evolution of an orbit (trajectory) with initial condition

$$P(0)=(q_1(0), q_2(0),\ldots,q_N(0), p_1(0), p_2(0),\ldots,p_N(0))$$

is governed by the Hamilton's equations of motion

$$\frac{dp_i}{dt} = -\frac{\partial H}{\partial q_i} \quad , \quad \frac{dq_i}{dt} = \frac{\partial H}{\partial p_i}$$

Variational Equations

We use the notation $\mathbf{x} = (q_1, q_2, \ldots, q_N, p_1, p_2, \ldots, p_N)^T$. The **deviation vector** from a given orbit is denoted by

$$\mathbf{v} = (\delta x_1, \delta x_2, \ldots, \delta x_n)^T \text{ , with } n=2N$$

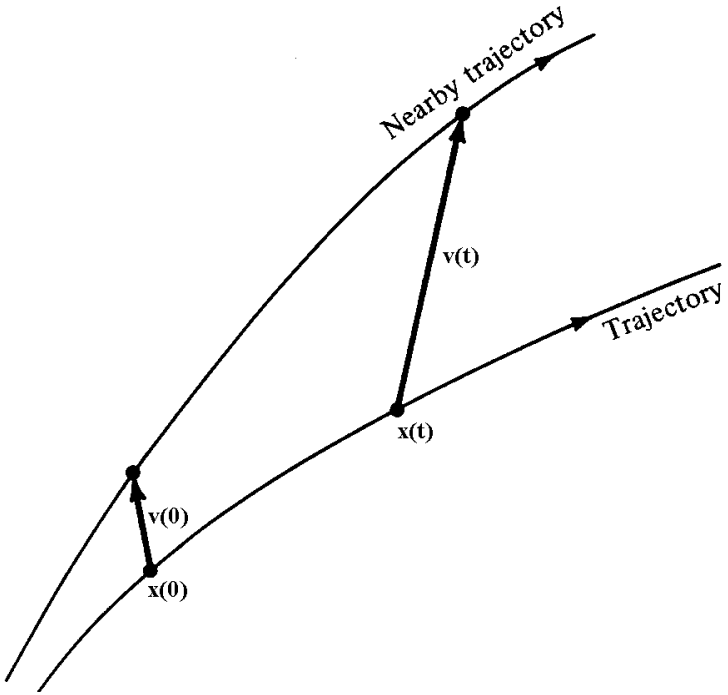

Benettin & Galgani, 1979, in Laval and Gressillon (eds.), op cit, 93

The time evolution of v is given by the so-called **variational equations:**

$$\frac{d\mathbf{v}}{dt} = -\mathbf{J} \cdot \mathbf{P} \cdot \mathbf{v}$$

where

$$\mathbf{J} = \begin{pmatrix} \mathbf{0}_N & -\mathbf{I}_N \\ \mathbf{I}_N & \mathbf{0}_N \end{pmatrix}, \quad \mathbf{P}_{ij} = \frac{\partial^2 H}{\partial x_i \partial x_j} \quad i, j = 1, 2, \ldots, n$$

Symplectic Maps

Consider an 2N-dimensional symplectic map T. In this case we have discrete time.

This is an area-preserving map whose Jacobian matrix

$$\mathbf{M} = \frac{\partial \mathbf{T}}{\partial \mathbf{x}} = \begin{bmatrix} \frac{\partial T_1}{\partial x_1} & \frac{\partial T_1}{\partial x_2} & \cdots & \frac{\partial T_1}{\partial x_{2N}} \\ \frac{\partial T_2}{\partial x_1} & \frac{\partial T_2}{\partial x_2} & \cdots & \frac{\partial T_2}{\partial x_{2N}} \\ \vdots & \vdots & & \vdots \\ \frac{\partial T_{2N}}{\partial x_1} & \frac{\partial T_{2N}}{\partial x_2} & \cdots & \frac{\partial T_{2N}}{\partial x_{2N}} \end{bmatrix}$$

satisfies

$$\mathbf{M}^{\mathrm{T}} \cdot \mathbf{J}_{2N} \cdot \mathbf{M} = \mathbf{J}_{2N}$$

Symplectic Maps

The evolution of an orbit with initial condition

$$P(0)=(x_1(0), x_2(0),\ldots,x_{2N}(0))$$

is governed by the equations of map T

$$P(i+1)=T\,P(i)\ ,\ \ i=0,1,2,\ldots$$

The evolution of an initial deviation vector

$$v(0) = (\delta x_1(0), \delta x_2(0),\ldots, \delta x_{2N}(0))$$

is given by the corresponding tangent map

$$v(i+1) = \left.\frac{\partial T}{\partial P}\right|_i \cdot v(i)\ ,\ i = 0, 1, 2, \ldots$$

Lyapunov Exponents

Roughly speaking, the Lyapunov exponents of a given orbit characterize the mean exponential rate of divergence of trajectories surrounding it.

Consider an orbit in the 2N-dimensional phase space with initial condition x(0) and an initial deviation vector from it v(0). Then the mean exponential rate of divergence is:

$$\sigma(x(0), v(0)) = \lim_{t \to \infty} \frac{1}{t} \ln \frac{\|v(t)\|}{\|v(0)\|}$$

Maximum Lyapunov Exponent

$\sigma_1 = 0 \rightarrow$ Regular motion

$\sigma_1 \neq 0 \rightarrow$ Chaotic motion

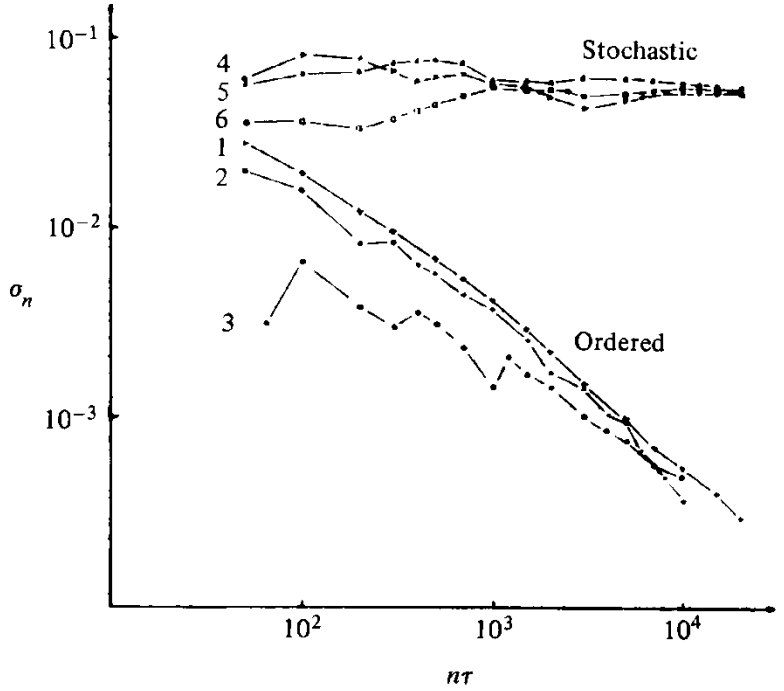

Figure 5.7. Behavior of σ_n at the intermediate energy $E = 0.125$ for initial points taken in the ordered (curves 1–3) or stochastic (curves 4–6) regions (after Benettin *et al.*, 1976).

If we start with more than one linearly independent deviation vectors they will align to the direction defined by the largest Lyapunov exponent for chaotic orbits.

The Smaller ALignment Index (SALI) method

Definition of Smaller Alignment Index (SALI)

Consider the 2N-dimensional phase space of a conservative dynamical system (symplectic map or Hamiltonian flow).

An orbit in that space with initial condition :

$$P(0)=(x_1(0), x_2(0),\ldots,x_{2N}(0))$$

and a deviation vector

$$v(0)=(\delta x_1(0), \delta x_2(0),\ldots, \delta x_{2N}(0))$$

The evolution in time (in maps the time is discrete and is equal to the number n of the iterations) of a deviation vector is defined by:

- **the variational equations (for Hamiltonian flows) and**
- **the equations of the tangent map (for mappings)**

Definition of SALI

We follow the evolution in time of two different initial deviation vectors ($v_1(0)$, $v_2(0)$), and define SALI (Ch.S. 2001, J. Phys. A) as:

$$SALI(t) = \min\left\{\left\|\hat{v}_1(t) + \hat{v}_2(t)\right\|, \left\|\hat{v}_1(t) - \hat{v}_2(t)\right\|\right\}$$

where

$$\hat{v}_1(t) = \frac{v_1(t)}{\left\|v_1(t)\right\|}$$

When the two vectors become collinear

$$SALI(t) \rightarrow 0$$

Behavior of SALI for chaotic motion

For chaotic orbits the two initially different deviation vectors tend to coincide with the direction defined by the maximum Lyapunov exponent.

Behavior of SALI for chaotic motion

For chaotic orbits the two initially different deviation vectors tend to coincide with the direction defined by the maximum Lyapunov exponent.

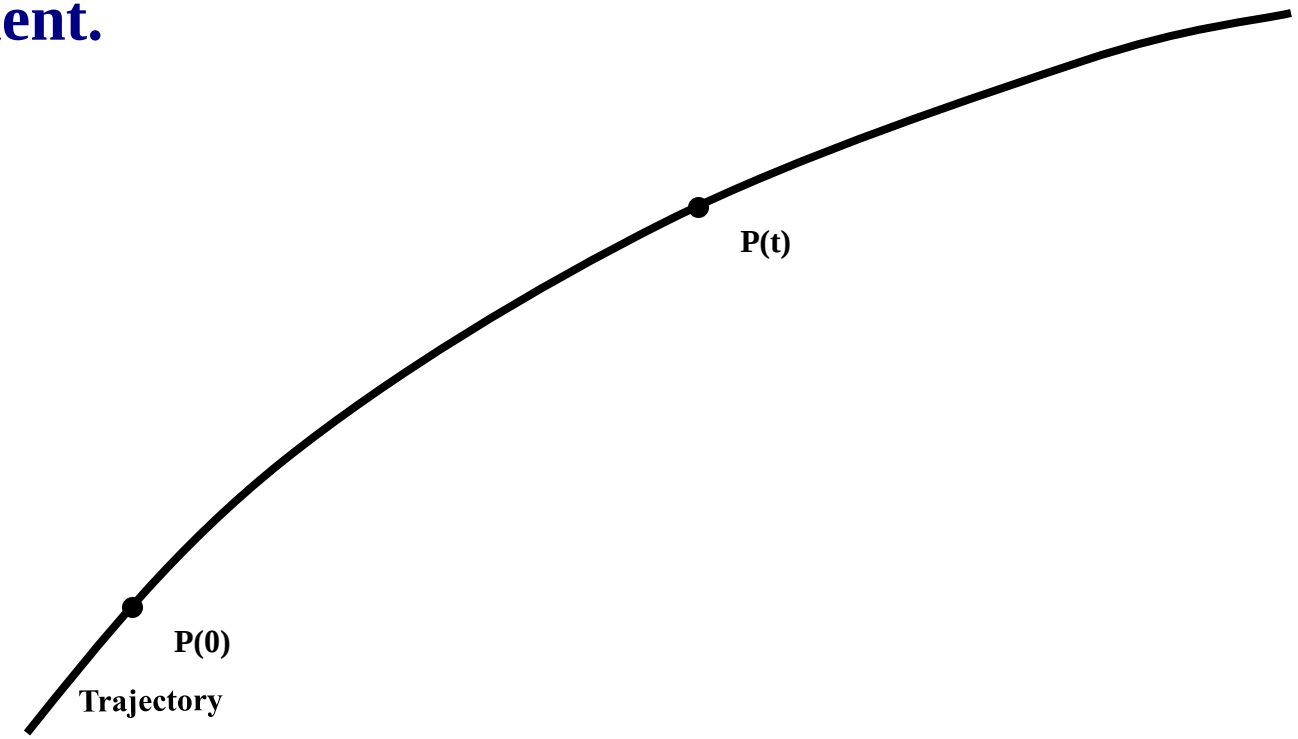

Behavior of SALI for chaotic motion

For chaotic orbits the two initially different deviation vectors tend to coincide with the direction defined by the maximum Lyapunov exponent.

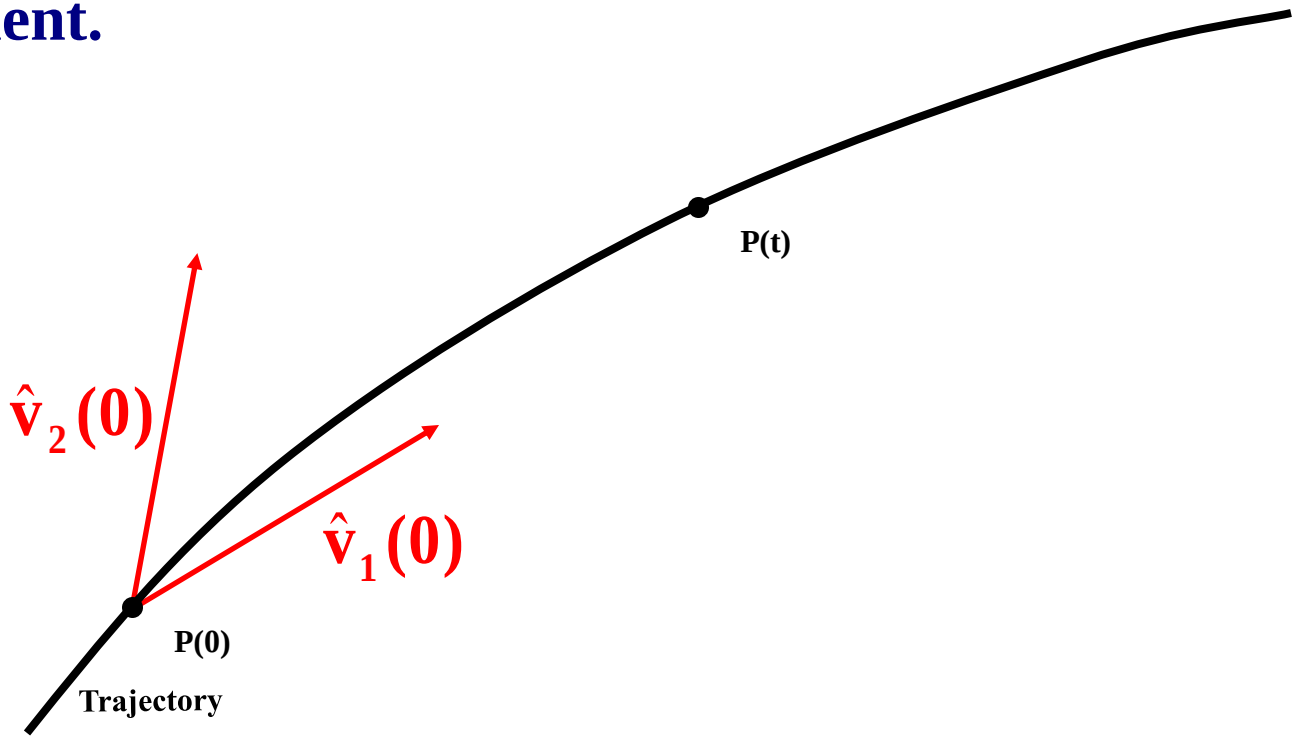

Behavior of SALI for chaotic motion

For chaotic orbits the two initially different deviation vectors tend to coincide with the direction defined by the maximum Lyapunov exponent.

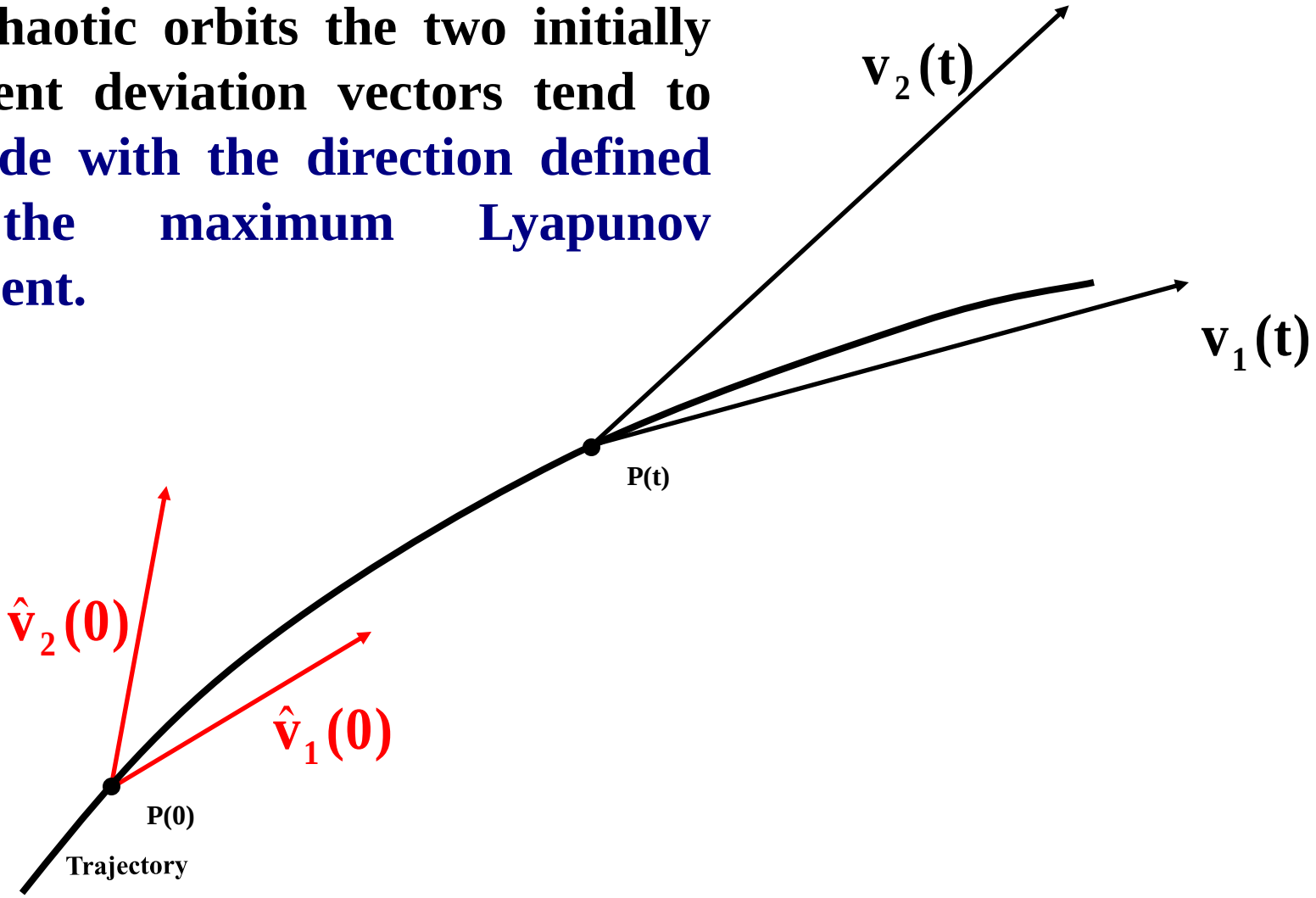

Behavior of SALI for chaotic motion

For chaotic orbits the two initially different deviation vectors tend to coincide with the direction defined by the maximum Lyapunov exponent.

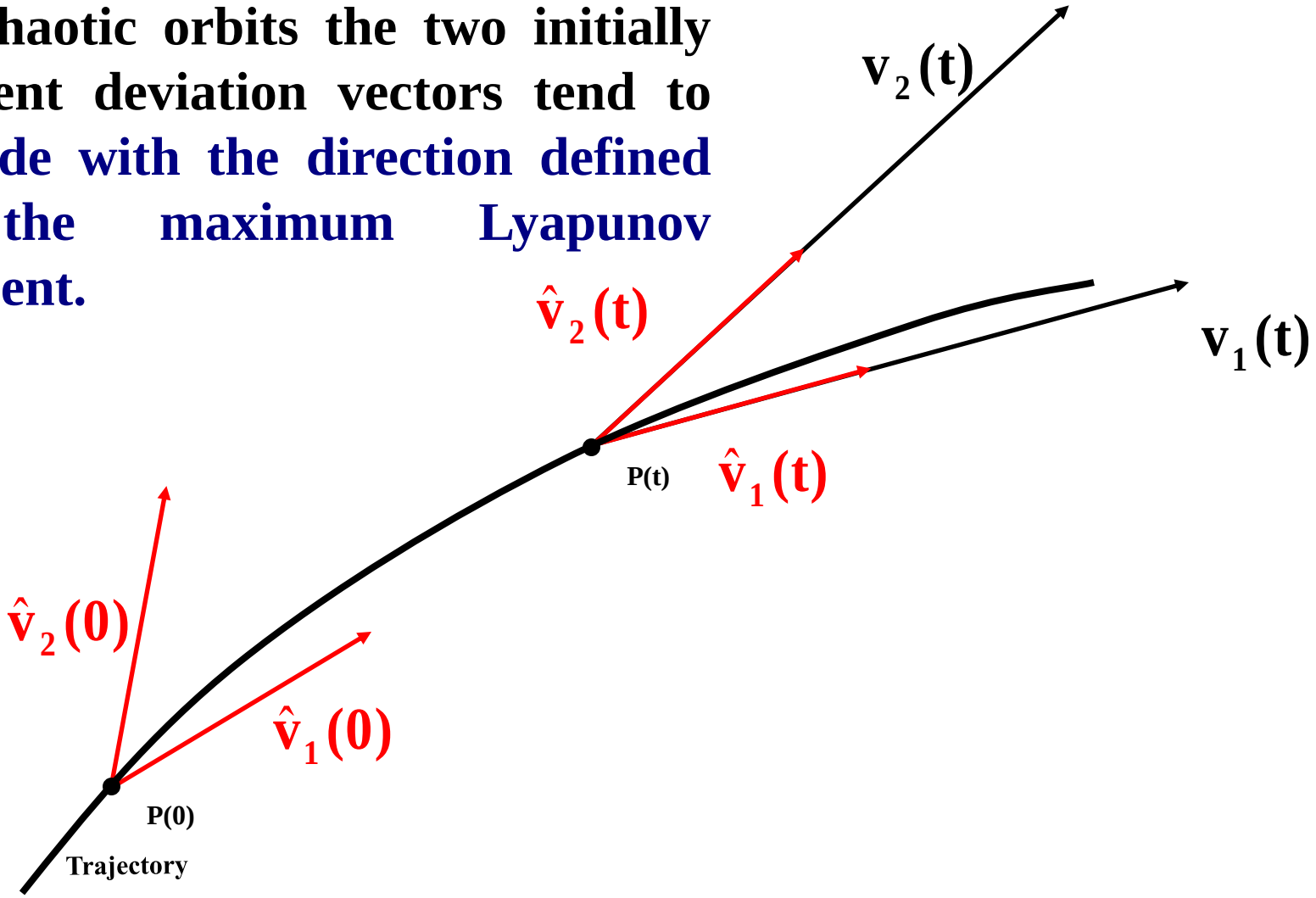

Behavior of SALI for chaotic motion

For chaotic orbits the two initially different deviation vectors tend to coincide with the direction defined by the maximum Lyapunov exponent.

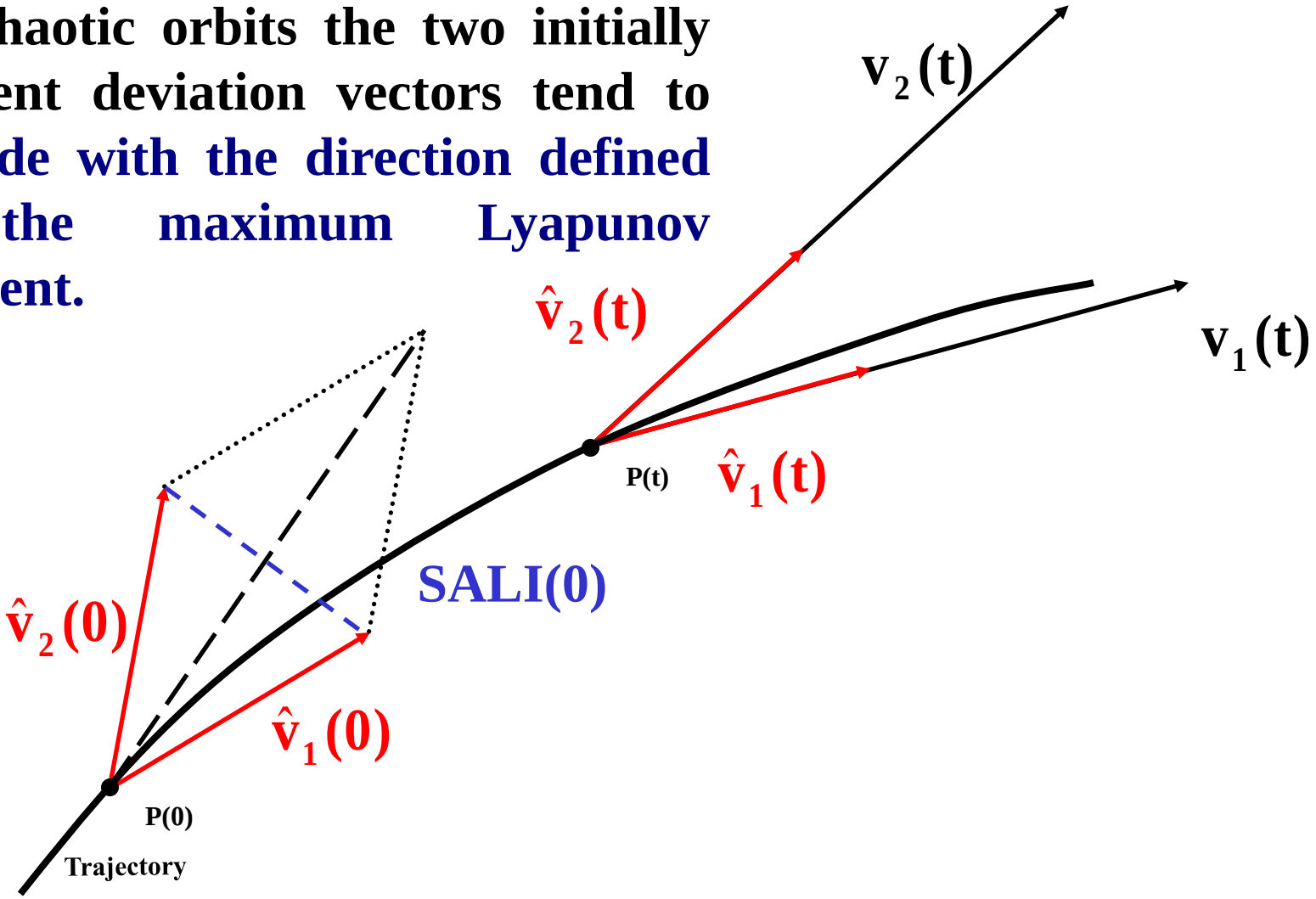

Behavior of SALI for chaotic motion

For chaotic orbits the two initially different deviation vectors tend to coincide with the direction defined by the maximum Lyapunov exponent.

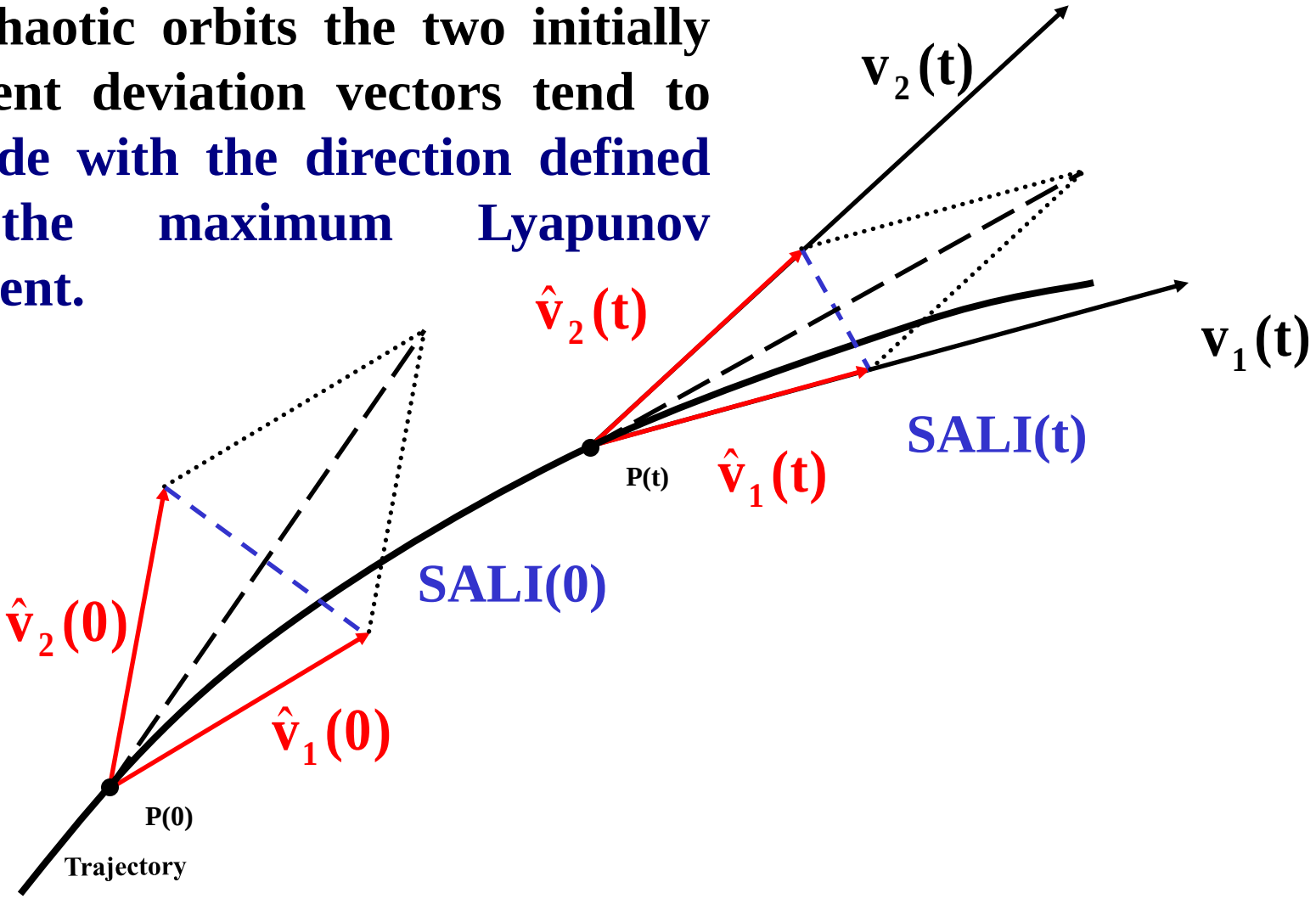

Behavior of SALI for chaotic motion

We test the validity of the approximation $SALI \propto e^{-(\sigma_1-\sigma_2)t}$ **(Ch.S., Antonopoulos, Bountis, Vrahatis, 2004, J. Phys. A) for a chaotic orbit of the 3D Hamiltonian**

$$H = \sum_{i=1}^{3} \frac{\omega_i}{2}(q_i^2 + p_i^2) + q_1^2 q_2 + q_1^2 q_3$$

with $\omega_1=1$, $\omega_2=1.4142$, $\omega_3=1.7321$, $H=0.09$

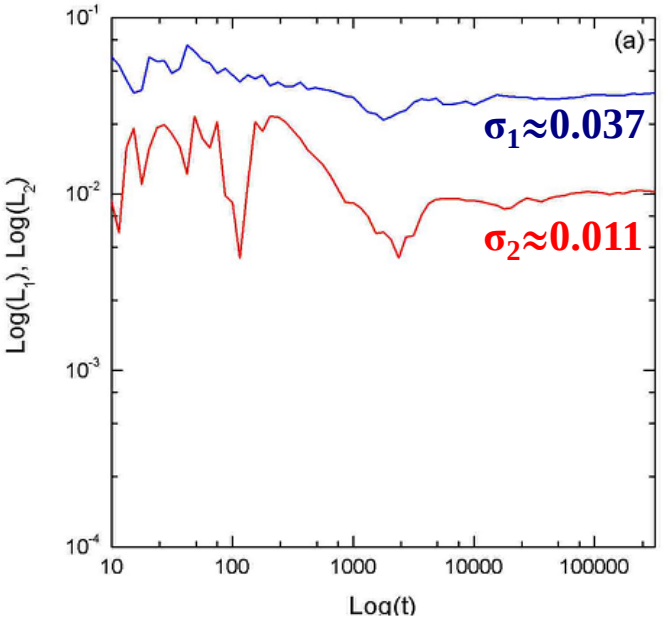

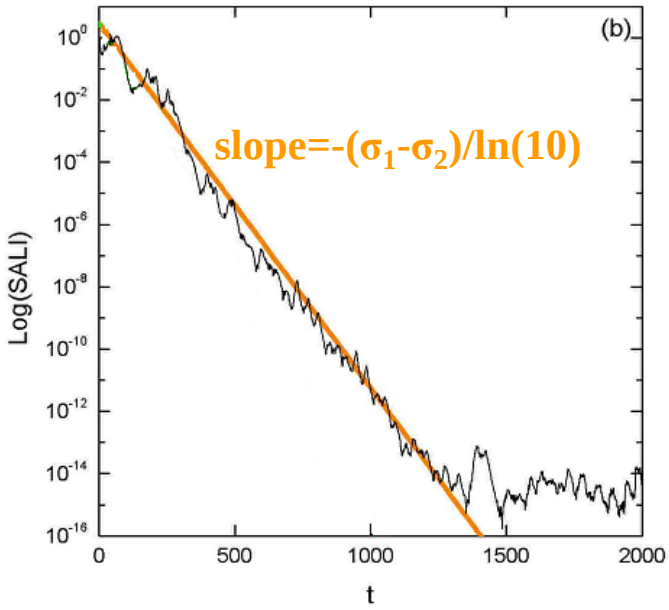

Behavior of SALI for regular motion

Regular motion occurs on a torus and two different initial deviation vectors become tangent to the torus, generally having different directions.

Behavior of SALI for regular motion

Regular motion occurs on a torus and two different initial deviation vectors become tangent to the torus, generally having different directions.

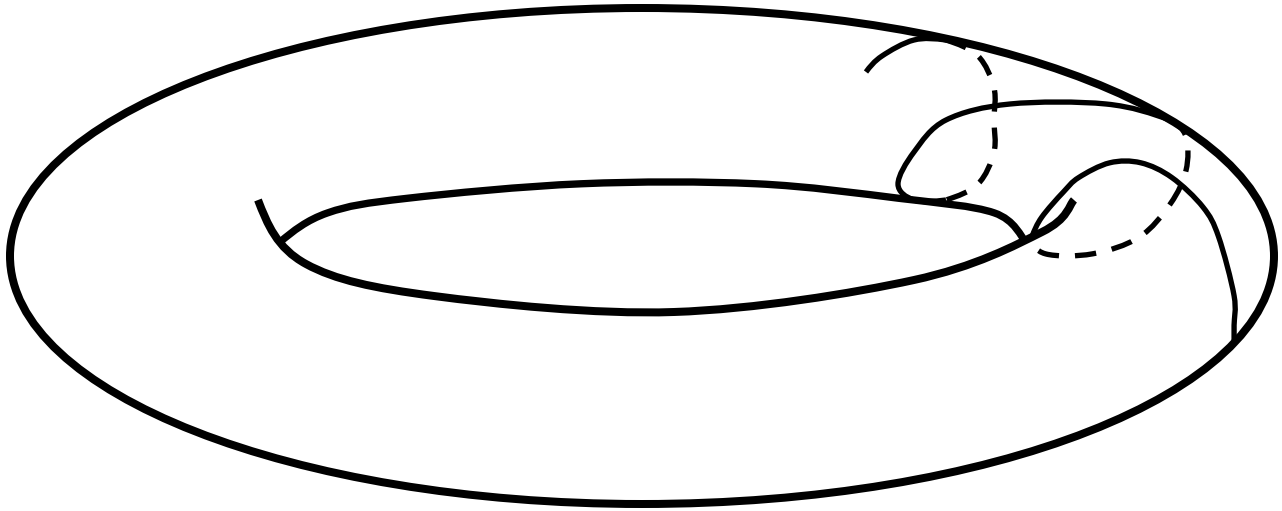

Behavior of SALI for regular motion

Regular motion occurs on a torus and two different initial deviation vectors become tangent to the torus, generally having different directions.

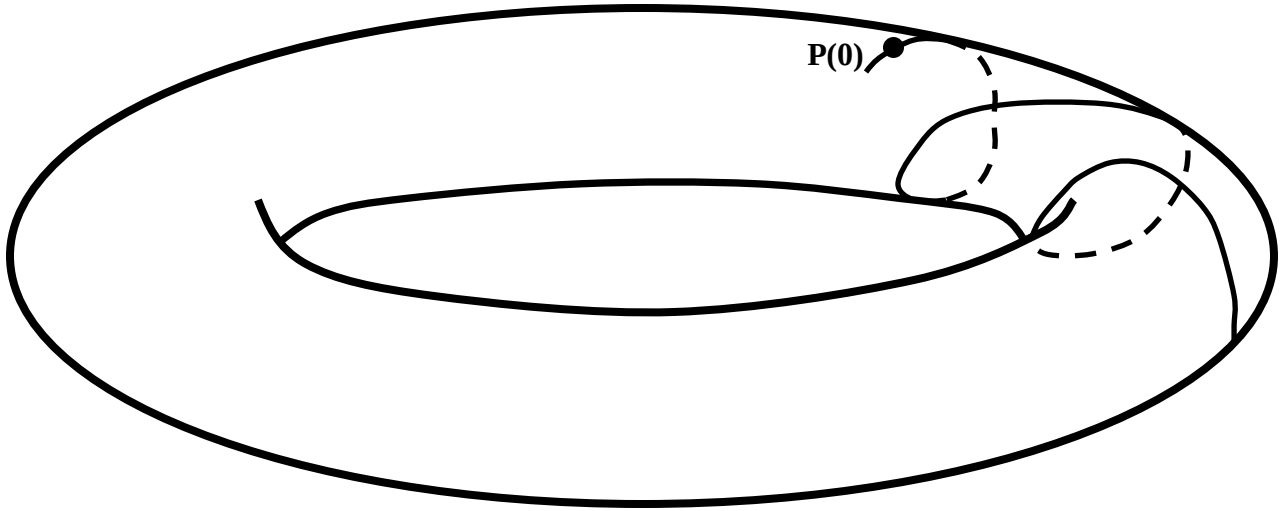

Behavior of SALI for regular motion

Regular motion occurs on a torus and two different initial deviation vectors become tangent to the torus, generally having different directions.

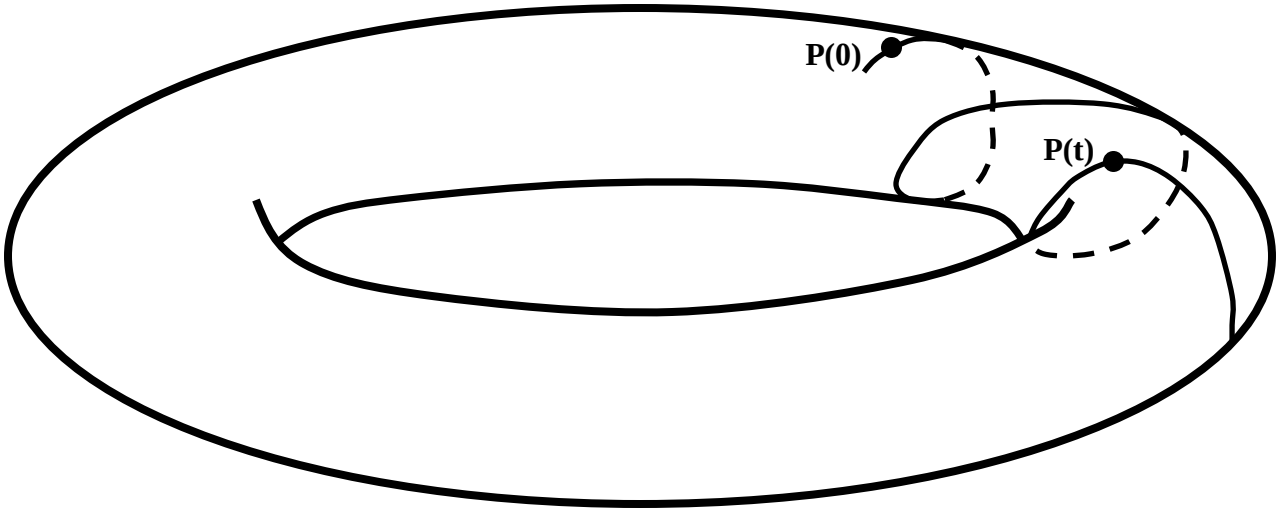

Behavior of SALI for regular motion

Regular motion occurs on a torus and two different initial deviation vectors become tangent to the torus, generally having different directions.

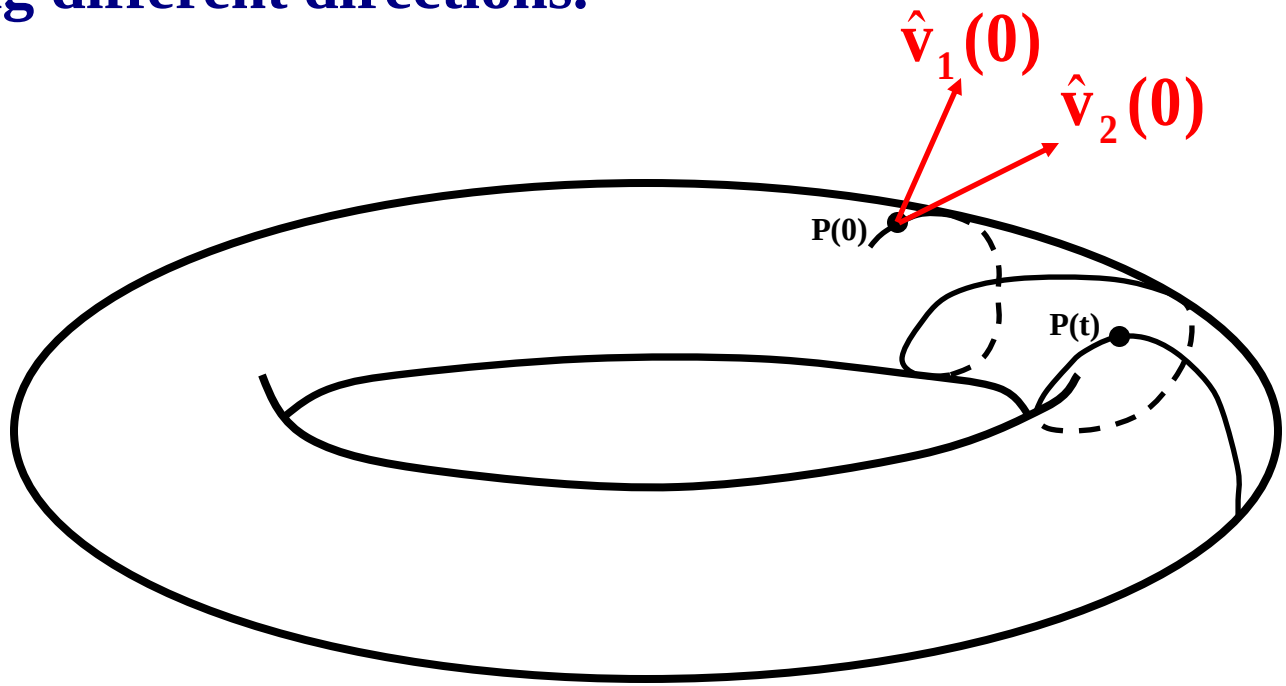

Behavior of SALI for regular motion

Regular motion occurs on a torus and two different initial deviation vectors become tangent to the torus, generally having different directions.

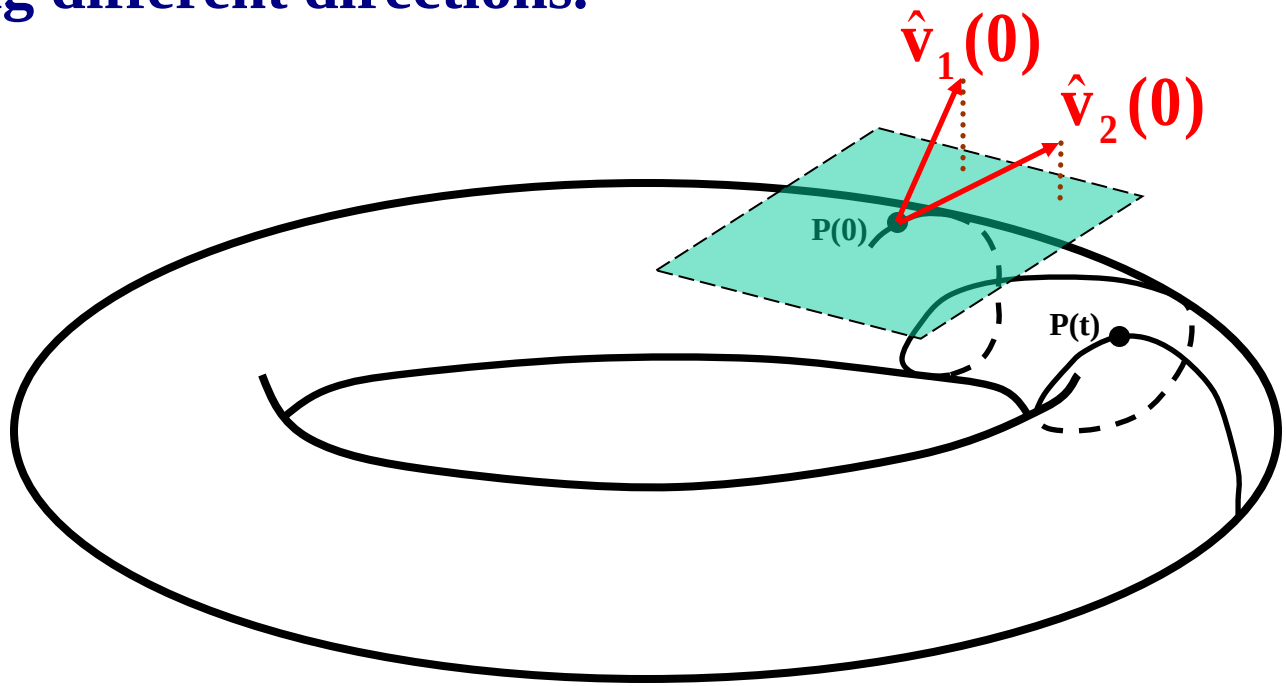

Behavior of SALI for regular motion

Regular motion occurs on a torus and two different initial deviation vectors become tangent to the torus, generally having different directions.

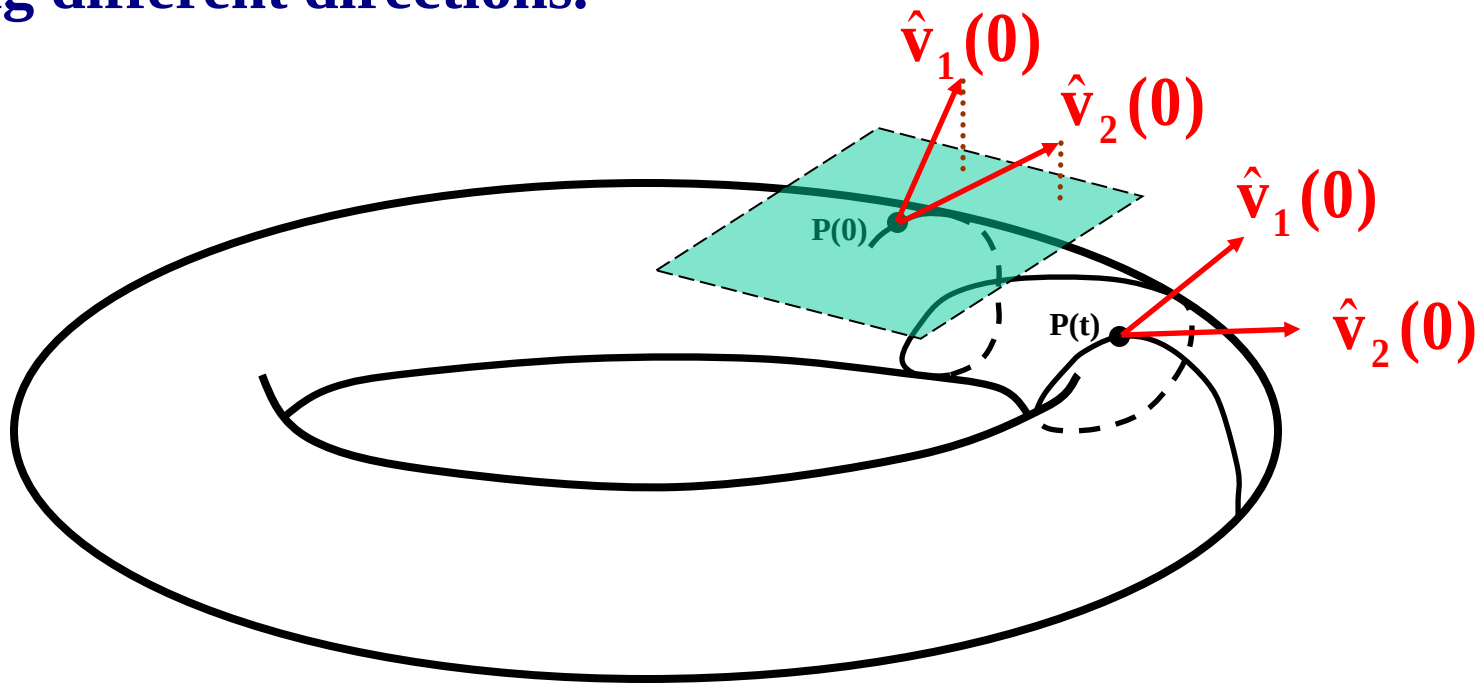

Behavior of SALI for regular motion

Regular motion occurs on a torus and two different initial deviation vectors become tangent to the torus, generally having different directions.

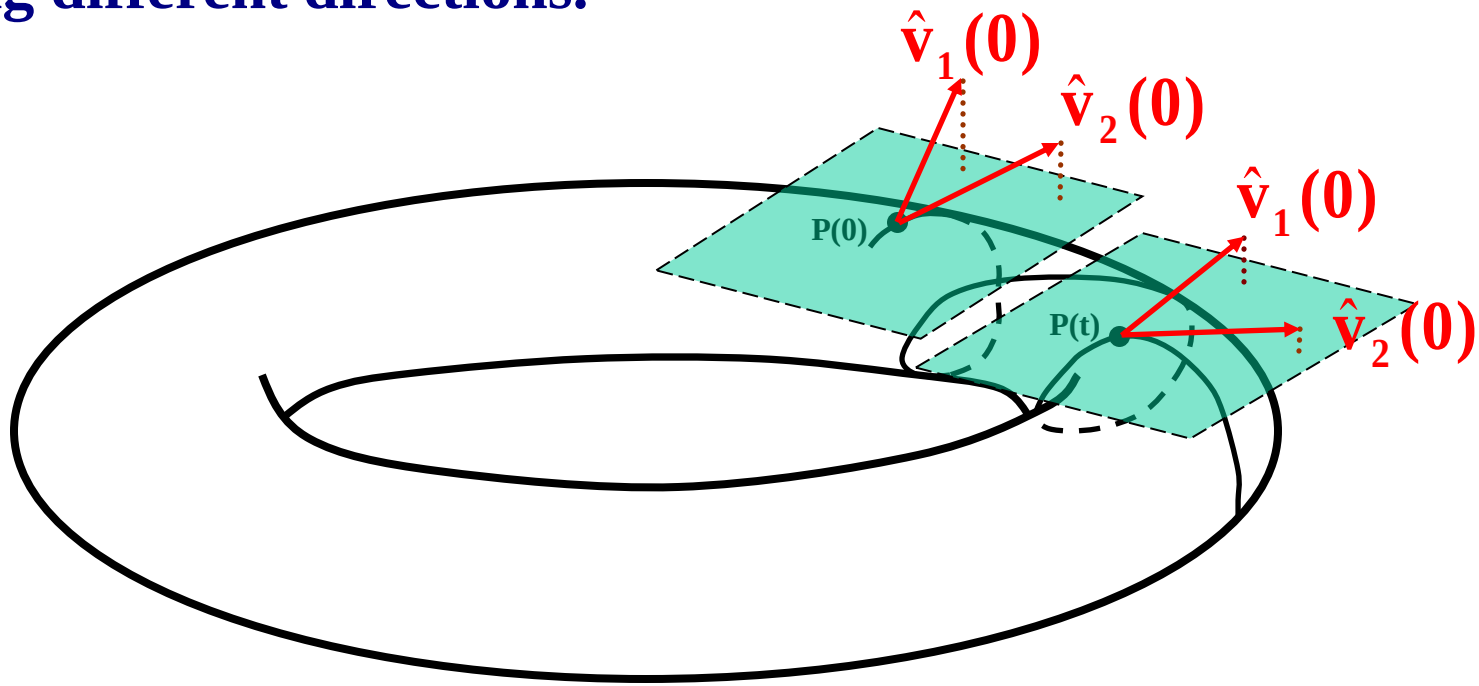

Applications – Hénon-Heiles system

As an example, we consider the 2D Hénon-Heiles system:

$$H_2 = \frac{1}{2}(p_x^2 + p_y^2) + \frac{1}{2}(x^2 + y^2) + x^2 y - \frac{1}{3}y^3$$

For E=1/8 we consider the orbits with initial conditions:
Regular orbit, x=0, y=0.55, p_x=0.2417, p_y=0
Chaotic orbit, x=0, y=-0.016, p_x=0.49974, p_y=0
Chaotic orbit, x=0, y=-0.01344, p_x=0.49982, p_y=0

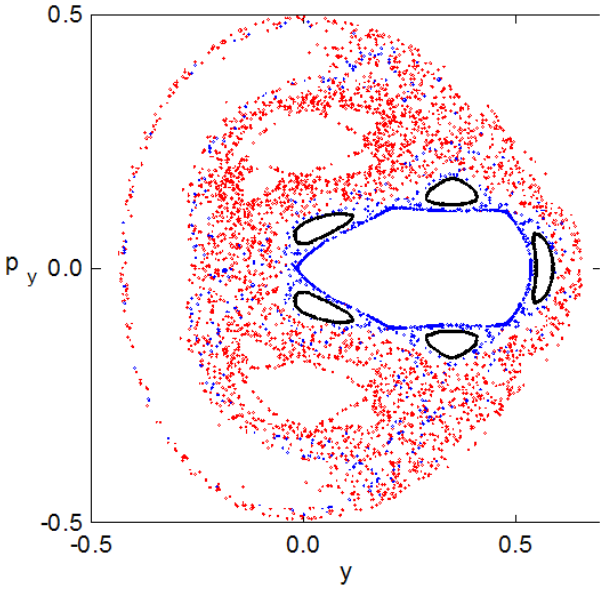

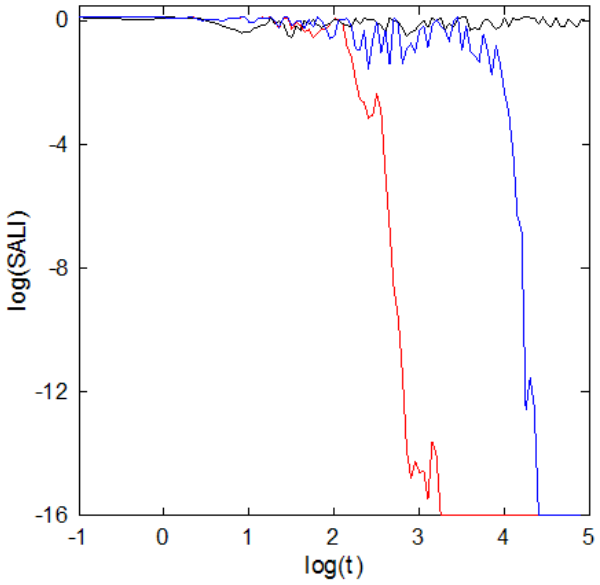

Applications – Hénon-Heiles system

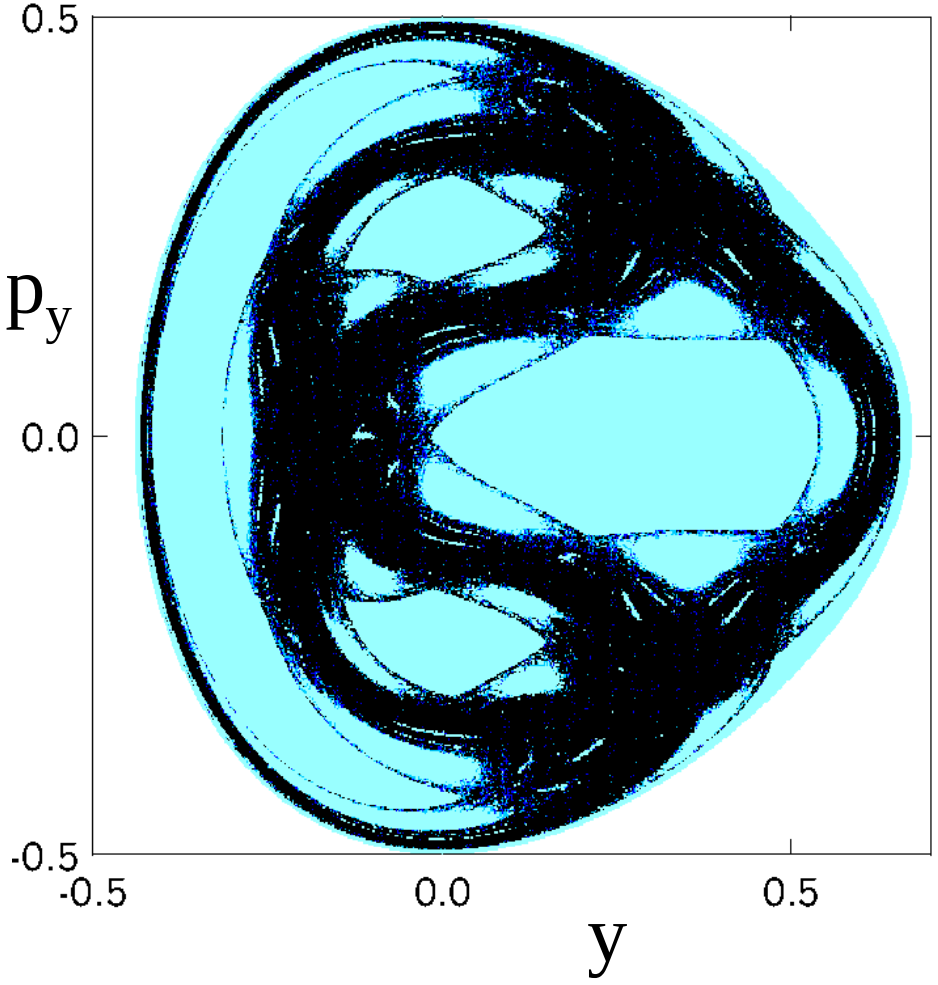

log(SALI) ≤ -12
-12 < log(SALI) ≤ -8
-8 < log(SALI) ≤ -4
-4 < log(SALI)

Applications – 4D map

$$
\begin{aligned}
x_1' &= x_1 + x_2 \\
x_2' &= x_2 - \nu \sin(x_1 + x_2) - \mu\,[1 - \cos(x_1 + x_2 + x_3 + x_4)] \\
x_3' &= x_3 + x_4 \\
x_4' &= x_4 - \kappa \sin(x_3 + x_4) - \mu\,[1 - \cos(x_1 + x_2 + x_3 + x_4)]
\end{aligned}
\qquad (\mathrm{mod}\ 2\pi)
$$

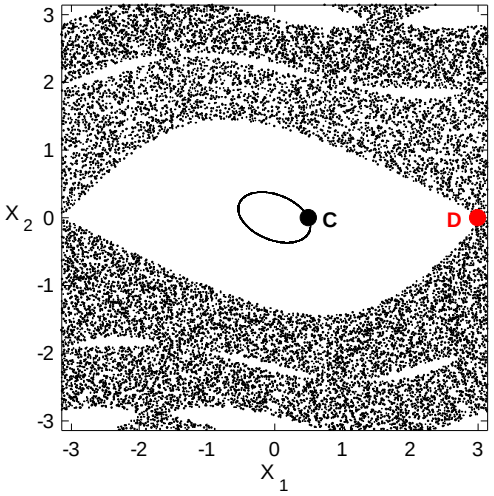

For ν=0.5, κ=0.1, μ=0.1 we consider the orbits:
regular orbit C *with initial conditions* $x_1=0.5$, $x_2=0$, $x_3=0.5$, $x_4=0$.
chaotic orbit D *with initial conditions* $x_1=3$, $x_2=0$, $x_3=0.5$, $x_4=0$.

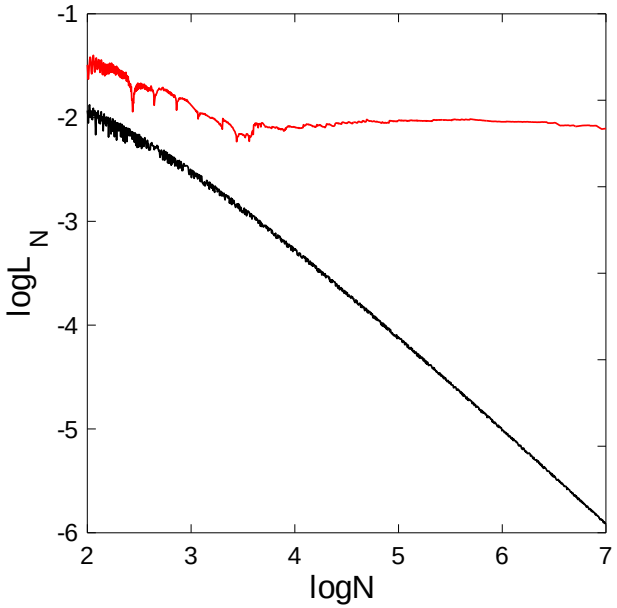

Applications – 4D map

$$
\begin{aligned}
x_1' &= x_1 + x_2 \\
x_2' &= x_2 - \nu \sin(x_1 + x_2) - \mu\,[1 - \cos(x_1 + x_2 + x_3 + x_4)] \\
x_3' &= x_3 + x_4 \\
x_4' &= x_4 - \kappa \sin(x_3 + x_4) - \mu\,[1 - \cos(x_1 + x_2 + x_3 + x_4)]
\end{aligned}
\qquad (\mathrm{mod}\ 2\pi)
$$

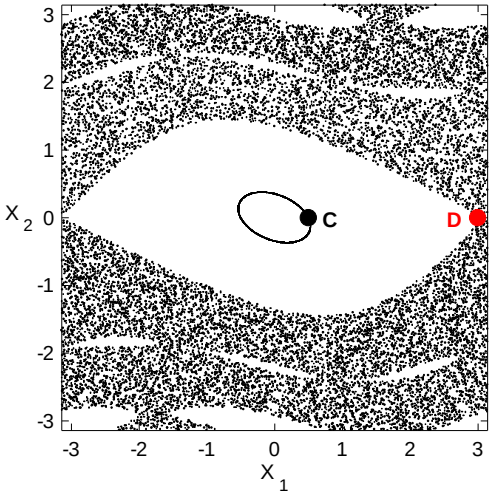

For ν=0.5, κ=0.1, μ=0.1 we consider the orbits:
regular orbit C *with initial conditions* $x_1=0.5$, $x_2=0$, $x_3=0.5$, $x_4=0$.
chaotic orbit D *with initial conditions* $x_1=3$, $x_2=0$, $x_3=0.5$, $x_4=0$.

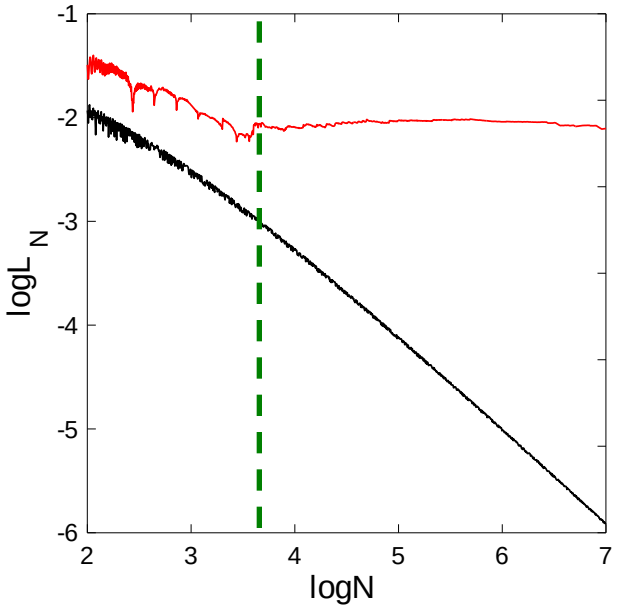

Applications – 4D map

$$
\begin{aligned}
x_1' &= x_1 + x_2 \\
x_2' &= x_2 - \nu \sin(x_1 + x_2) - \mu\,[1 - \cos(x_1 + x_2 + x_3 + x_4)] \\
x_3' &= x_3 + x_4 \\
x_4' &= x_4 - \kappa \sin(x_3 + x_4) - \mu\,[1 - \cos(x_1 + x_2 + x_3 + x_4)]
\end{aligned}
\qquad (\mathrm{mod}\ 2\pi)
$$

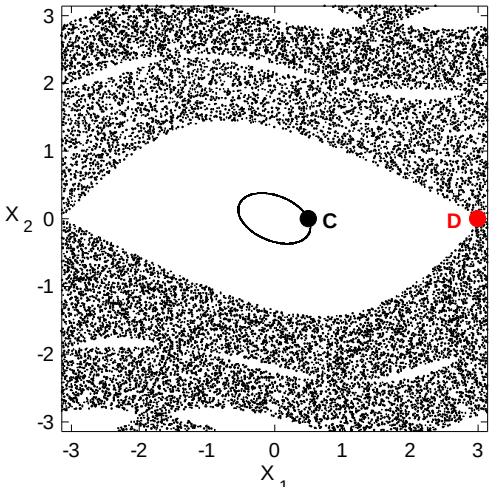

For ν=0.5, κ=0.1, μ=0.1 we consider the orbits:
regular orbit C *with initial conditions* $x_1=0.5$, $x_2=0$, $x_3=0.5$, $x_4=0$.
chaotic orbit D *with initial conditions* $x_1=3$, $x_2=0$, $x_3=0.5$, $x_4=0$.

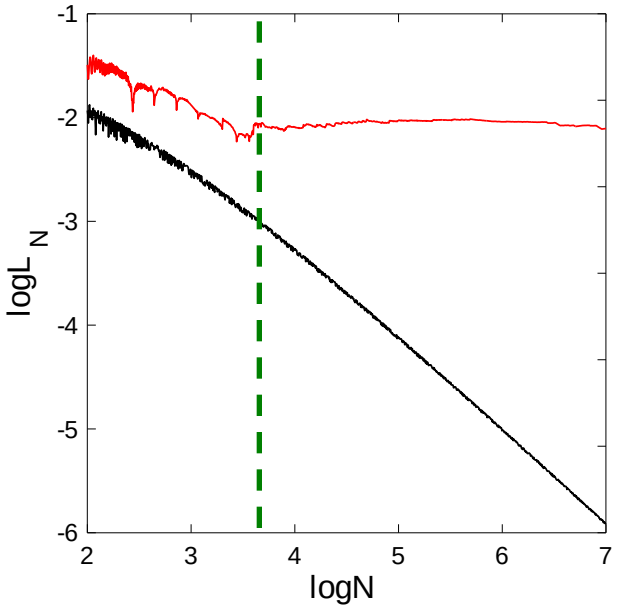

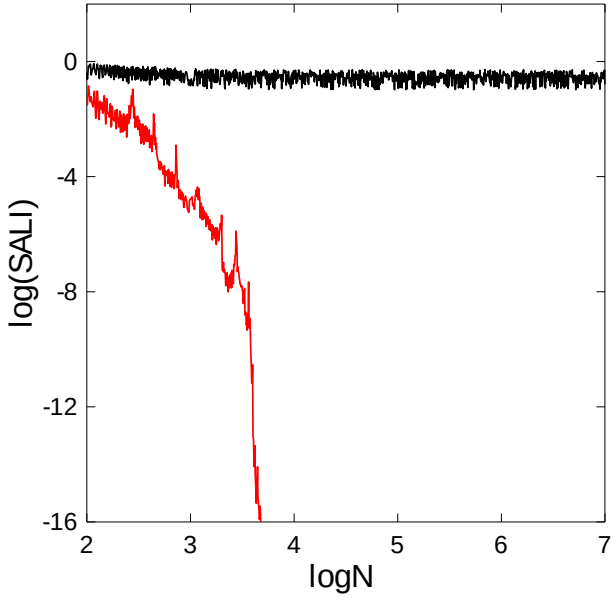

Applications – 4D map

$$
\begin{aligned}
x_1' &= x_1 + x_2 \\
x_2' &= x_2 - \nu \sin(x_1 + x_2) - \mu\,[1 - \cos(x_1 + x_2 + x_3 + x_4)] \\
x_3' &= x_3 + x_4 \\
x_4' &= x_4 - \kappa \sin(x_3 + x_4) - \mu\,[1 - \cos(x_1 + x_2 + x_3 + x_4)]
\end{aligned}
\qquad (\mathrm{mod}\ 2\pi)
$$

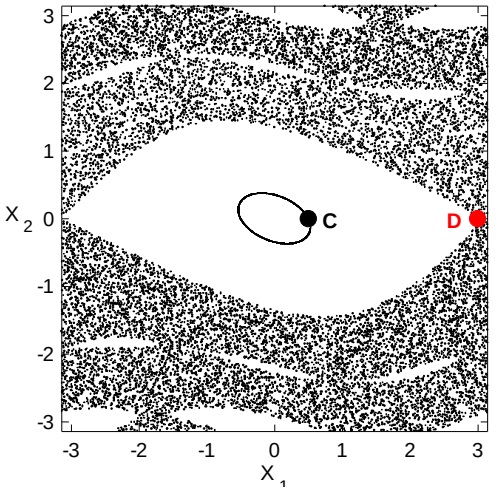

For ν=0.5, κ=0.1, μ=0.1 we consider the orbits:

regular orbit C *with initial conditions* $x_1=0.5$, $x_2=0$, $x_3=0.5$, $x_4=0$.

chaotic orbit D *with initial conditions* $x_1=3$, $x_2=0$, $x_3=0.5$, $x_4=0$.

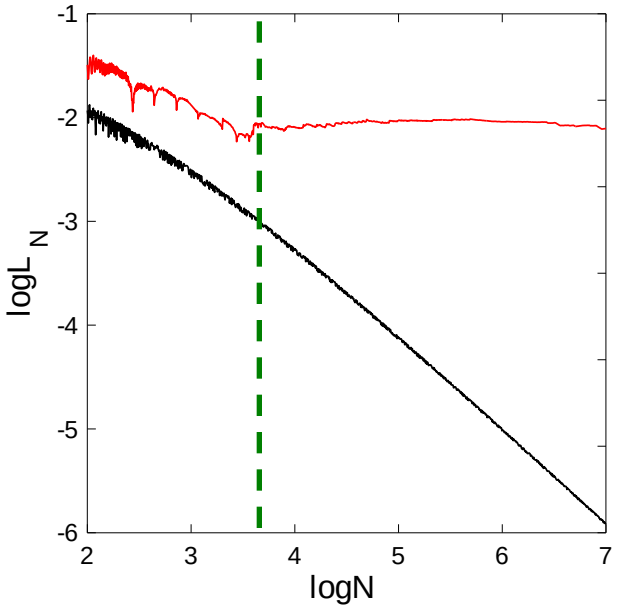

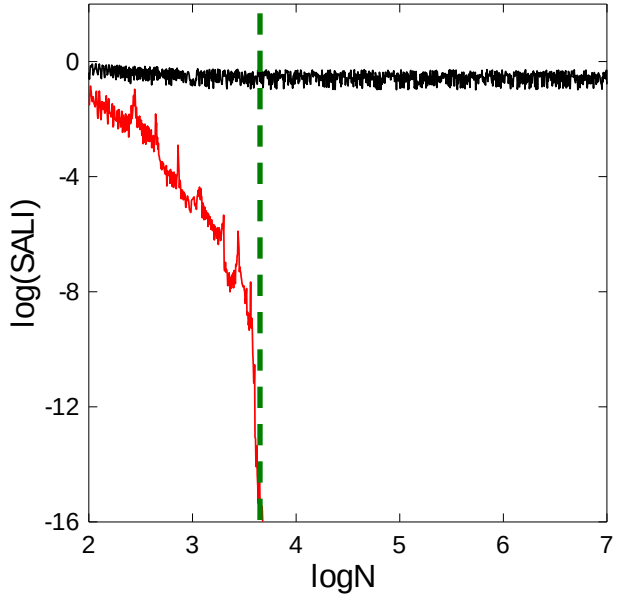

Applications – 2D map

$$x_1' = x_1 + x_2$$
$$x_2' = x_2 - \nu \sin(x_1 + x_2) \quad (\mathrm{mod}\ 2\pi)$$

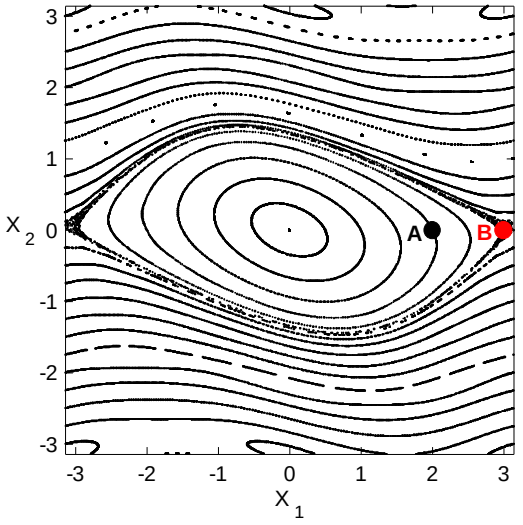

For ν=0.5 we consider the orbits:
regular orbit A *with initial conditions* $x_1=2$, $x_2=0$.
chaotic orbit B *with initial conditions* $x_1=3$, $x_2=0$.

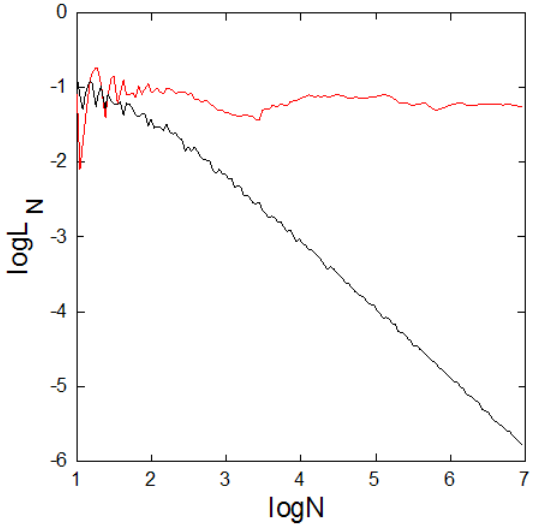

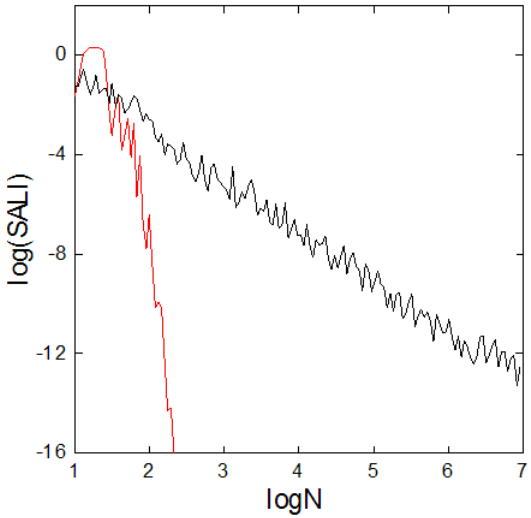

Behavior of SALI

2D maps

SALI→0 both for regular and chaotic orbits

following, however, completely different time rates which allows us to distinguish between the two cases.

Hamiltonian flows and multidimensional maps

SALI→0 for chaotic orbits

SALI→constant ≠ 0 for regular orbits

Questions

Can we generalize SALI so that the new index:

- **Can rapidly reveal the nature of chaotic orbits with $\sigma_1 \approx \sigma_2$ ($SALI \propto e^{-(\sigma 1 - \sigma 2)t}$)?**

- **Depends on several Lyapunov exponents for chaotic orbits?**

- **Exhibits power-law decay for regular orbits depending on the dimensionality of the tangent space of the reference orbit as for 2D maps?**

The Generalized ALignment Indices (GALIs) method

Definition of Generalized Alignment Index (GALI)

SALI effectively measures the ‘area’ of the parallelogram formed by the two deviation vectors.

Definition of Generalized Alignment Index (GALI)

SALI effectively measures the 'area' of the parallelogram formed by the two deviation vectors.

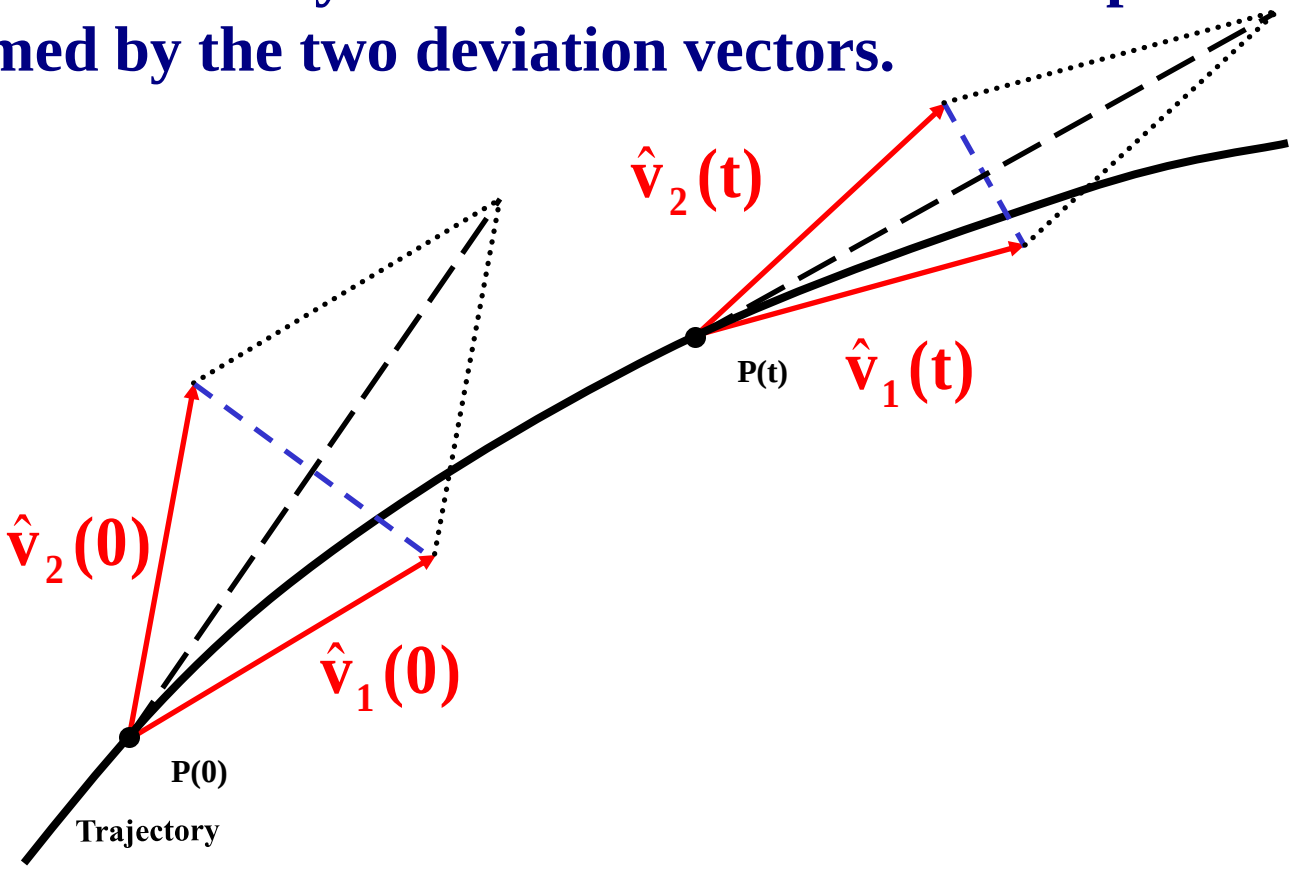

Definition of Generalized Alignment Index (GALI)

SALI effectively measures the 'area' of the parallelogram formed by the two deviation vectors.

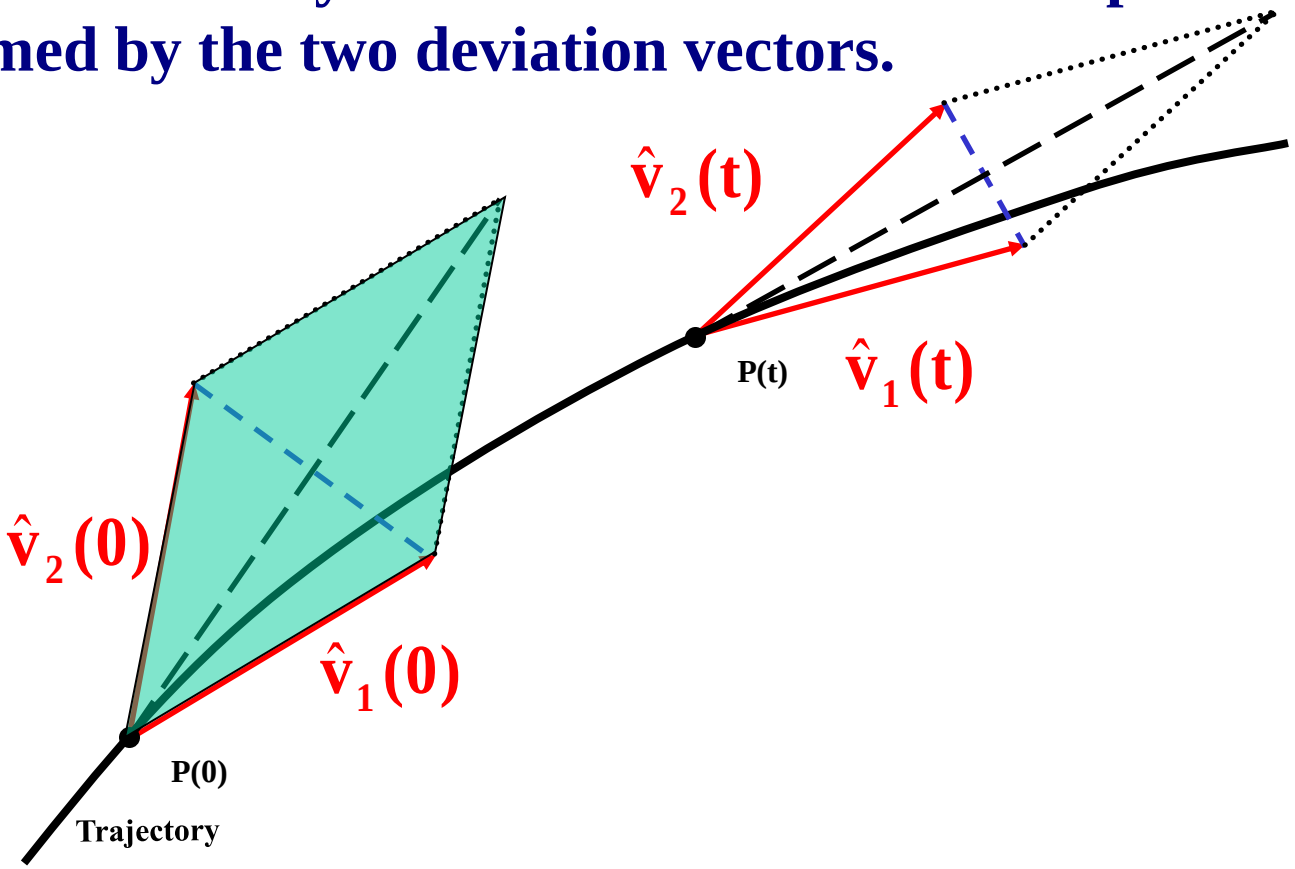

Definition of Generalized Alignment Index (GALI)

SALI effectively measures the 'area' of the parallelogram formed by the two deviation vectors.

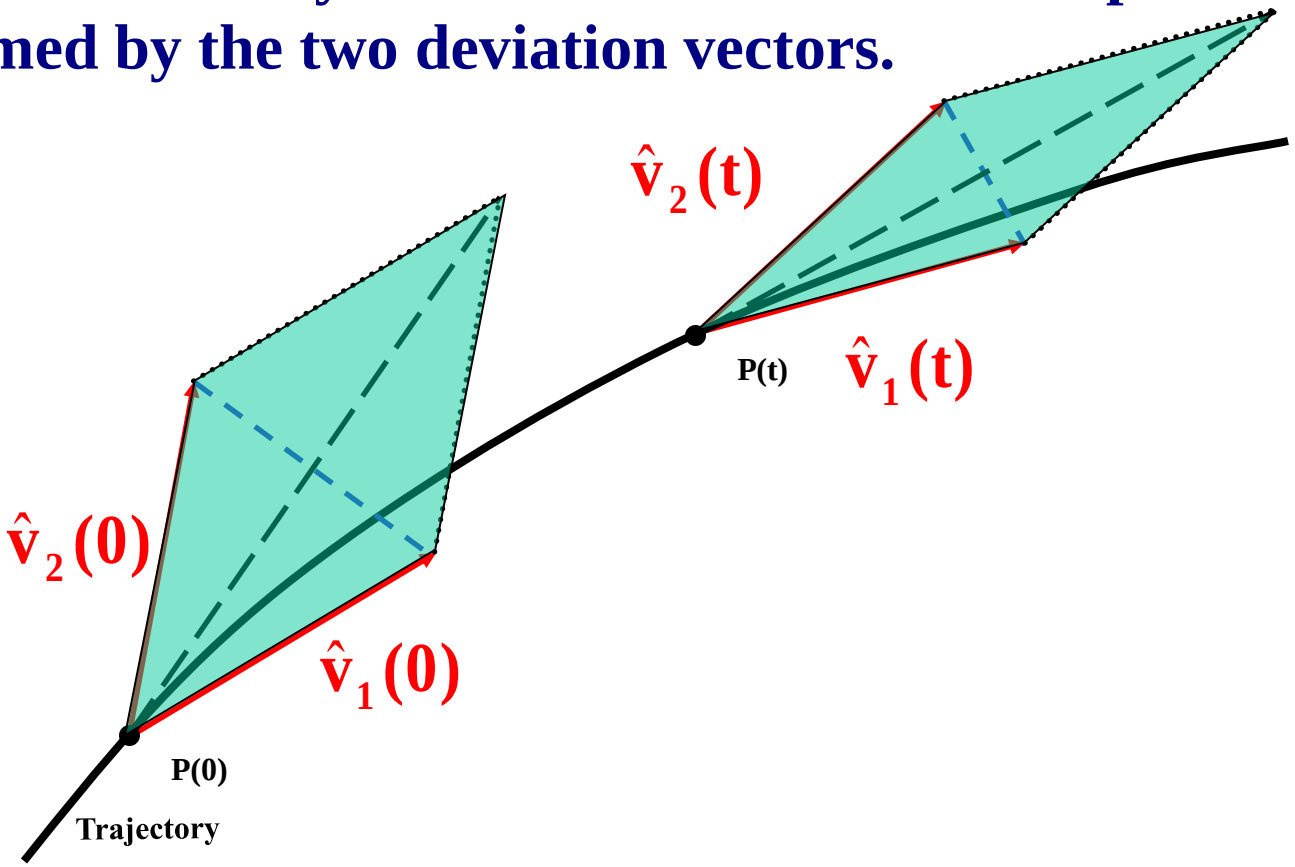

Definition of Generalized Alignment Index (GALI)

SALI effectively measures the 'area' of the parallelogram formed by the two deviation vectors.

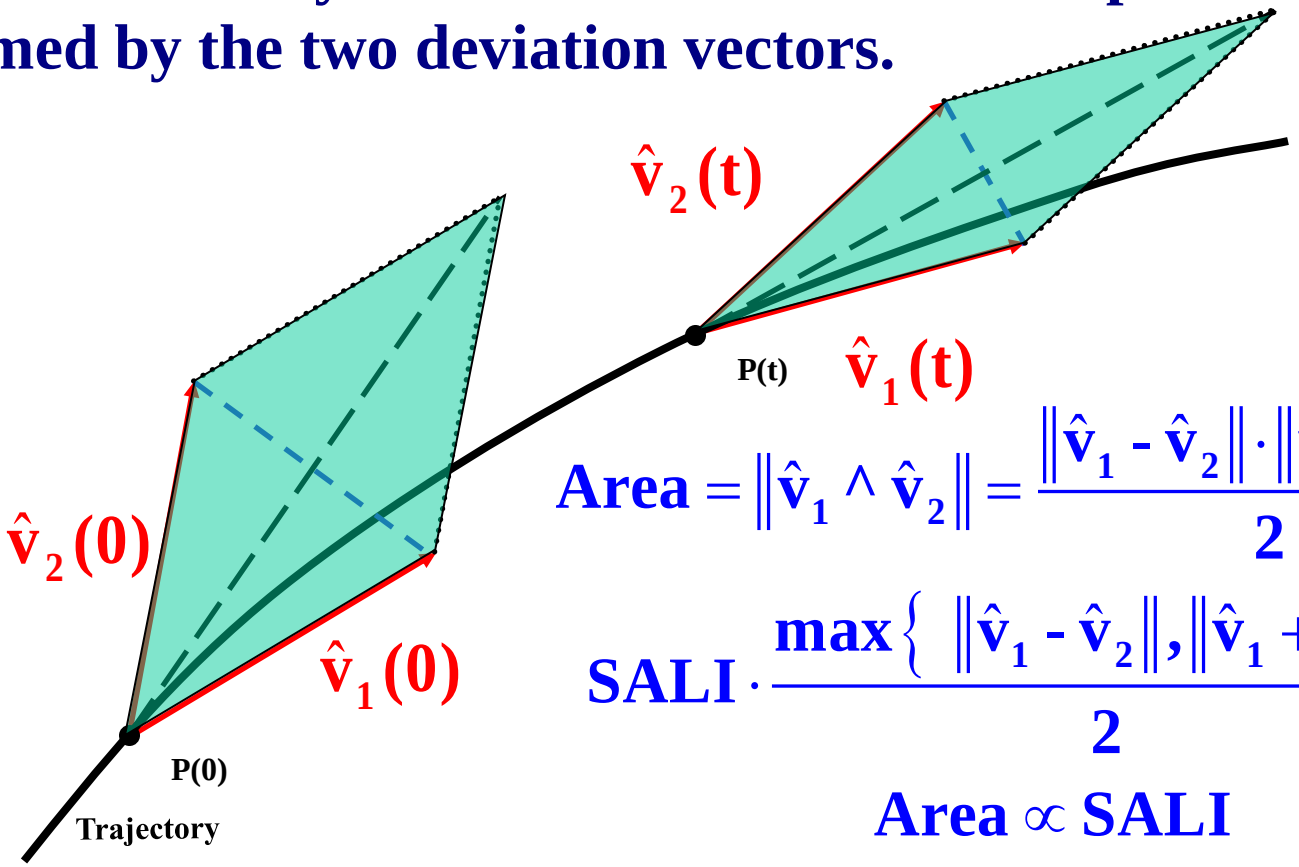

$$\text{Area} = \left\| \hat{v}_1 \wedge \hat{v}_2 \right\| = \frac{\left\| \hat{v}_1 - \hat{v}_2 \right\| \cdot \left\| \hat{v}_1 + \hat{v}_2 \right\|}{2} =$$

$$\text{SALI} \cdot \frac{\max\left\{ \left\| \hat{v}_1 - \hat{v}_2 \right\|, \left\| \hat{v}_1 + \hat{v}_2 \right\| \right\}}{2} \Rightarrow$$

$$\text{Area} \propto \text{SALI}$$

Definition of GALI

In the case of an N degree of freedom Hamiltonian system or a 2N symplectic map we follow the evolution of

k deviation vectors with $2 \leq k \leq 2N$,

and define (Ch.S., Bountis, Antonopoulos, 2007, Physica D) the Generalized Alignment Index (GALI) of order k :

$$GALI_k(t) = \left\| \hat{v}_1(t) \wedge \hat{v}_2(t) \wedge \ldots \wedge \hat{v}_k(t) \right\|$$

where

$$\hat{v}_1(t) = \frac{v_1(t)}{\left\| v_1(t) \right\|}$$

Behavior of $GALI_k$ for chaotic motion

$GALI_k$ $(2 \leq k \leq 2N)$ tends exponentially to zero with exponents that involve the values of the first k largest Lyapunov exponents $\sigma_1, \sigma_2, \ldots, \sigma_k$:

$$GALI_k(t) \propto e^{-\left[(\sigma_1-\sigma_2)+(\sigma_1-\sigma_3)+\ldots+(\sigma_1-\sigma_k)\right]t}$$

The above relation is valid even if some Lyapunov exponents are equal, or very close to each other.

Behavior of $GALI_k$ for chaotic motion

2D Hamiltonian (Hénon-Heiles system)

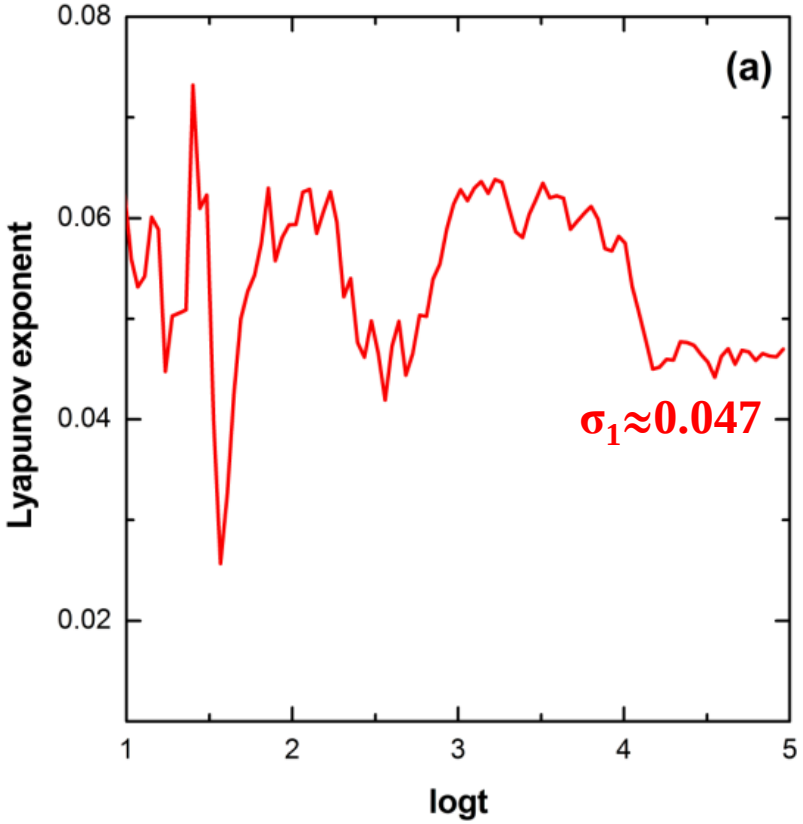

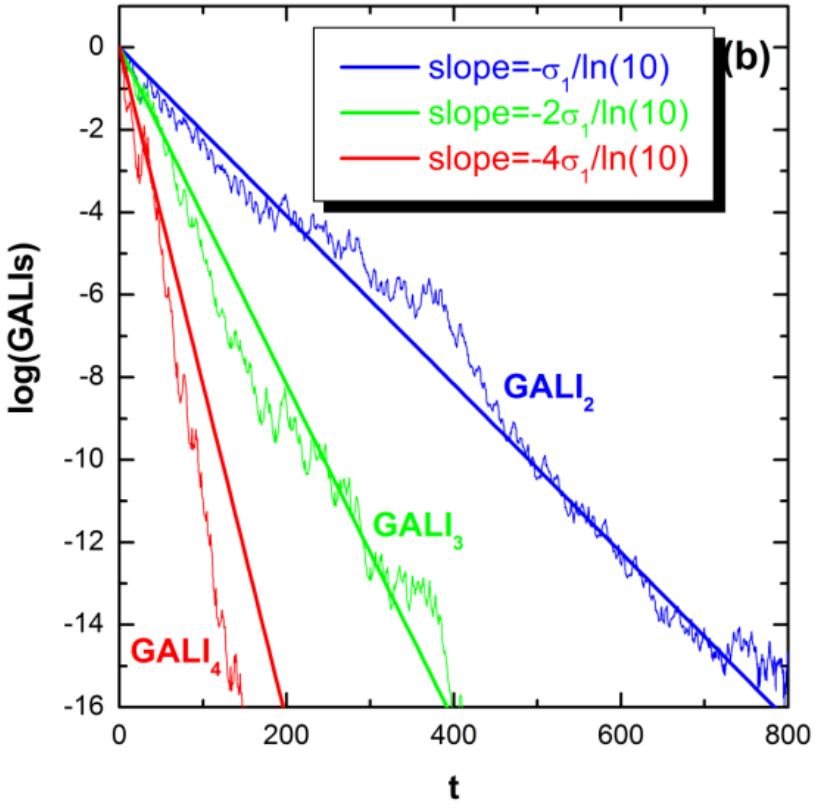

Behavior of $GALI_k$ for chaotic motion

N particles Fermi-Pasta-Ulam (FPU) system:

$$H = \frac{1}{2}\sum_{i=1}^{N} p_i^2 + \sum_{i=0}^{N}\left[\frac{1}{2}(q_{i+1} - q_i)^2 + \frac{\beta}{4}(q_{i+1} - q_i)^4\right]$$

with fixed boundary conditions, N=8 and β=1.5.

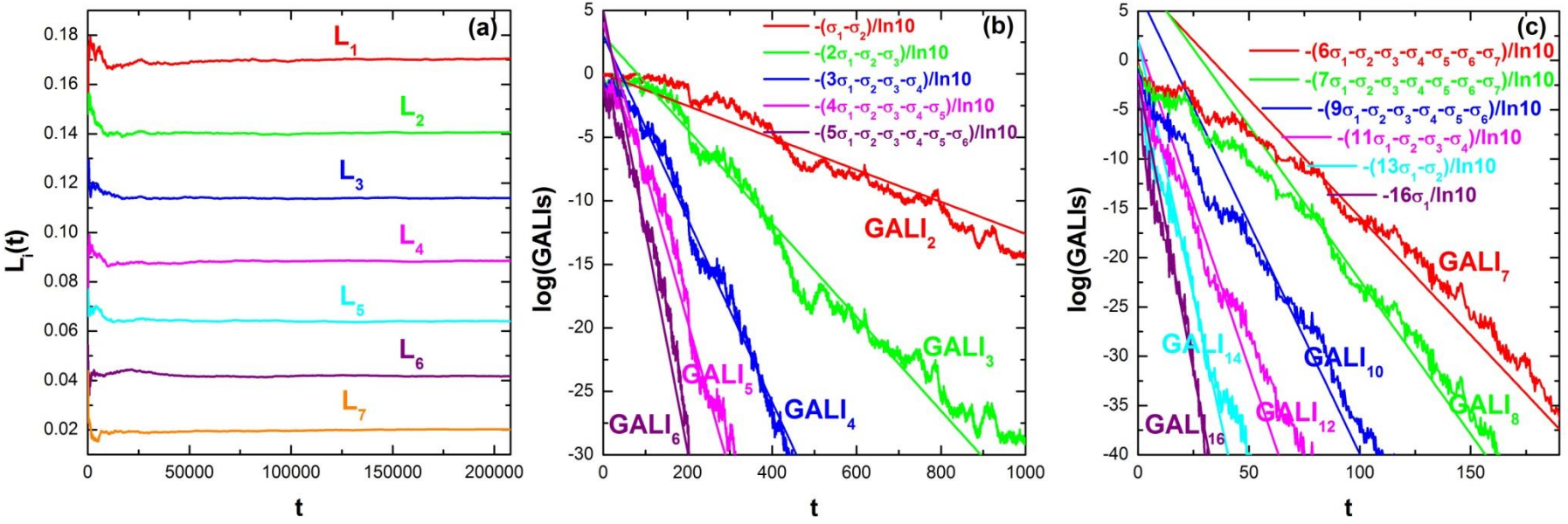

Behavior of $GALI_k$ for regular motion

If the motion occurs on an s-dimensional torus with $s \leq N$ then the behavior of $GALI_k$ is given by (Ch.S., Bountis, Antonopoulos, 2008, Eur. Phys. J. Sp. Top.):

$$GALI_k(t) \propto \begin{cases} \text{constant} & \text{if} \quad 2 \leq k \leq s \\ \dfrac{1}{t^{k-s}} & \text{if} \quad s < k \leq 2N - s \\ \dfrac{1}{t^{2(k-N)}} & \text{if} \quad 2N - s < k \leq 2N \end{cases}$$

while in the common case with s=N we have :

$$GALI_k(t) \propto \begin{cases} \text{constant} & \text{if} \quad 2 \leq k \leq N \\ \dfrac{1}{t^{2(k-N)}} & \text{if} \quad N < k \leq 2N \end{cases}$$

Behavior of $GALI_k$ for regular motion

N=8 FPU system: The unperturbed Hamiltonian (β=0) is written as a sum of the so-called **harmonic energies E_i:**

$$E_i = \frac{1}{2}\left(P_i^2 + \omega_i^2 Q_i^2\right),\ i = 1,...,N$$

with:

$$Q_i = \sqrt{\frac{2}{N+1}}\sum_{k=1}^{N} q_k \sin\left(\frac{ki\pi}{N+1}\right),\ P_i = \sqrt{\frac{2}{N+1}}\sum_{k=1}^{N} p_k \sin\left(\frac{ki\pi}{N+1}\right),\ \omega_i = 2\sin\left(\frac{i\pi}{2(N+1)}\right)$$

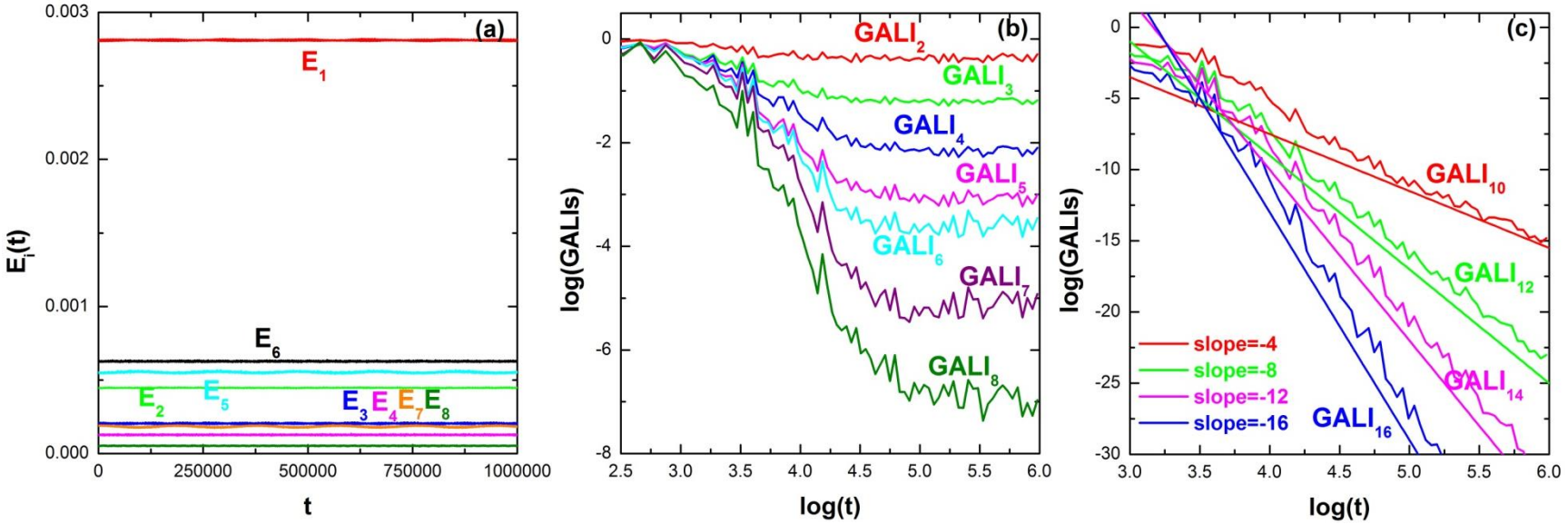

Global dynamics

- **$GALI_2$ (practically equivalent to the use of SALI)**
- **$GALI_N$**

Chaotic motion: $GALI_N \rightarrow 0$ (exponential decay)

Regular motion: $GALI_N \rightarrow$ constant$\neq 0$

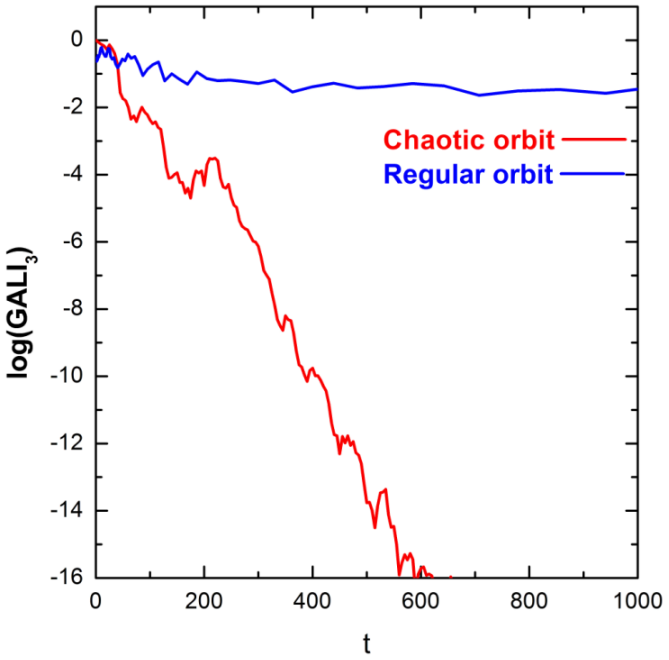

3D Hamiltonian

Subspace $q_3=p_3=0$, $p_2 \geq 0$ for t=1000.

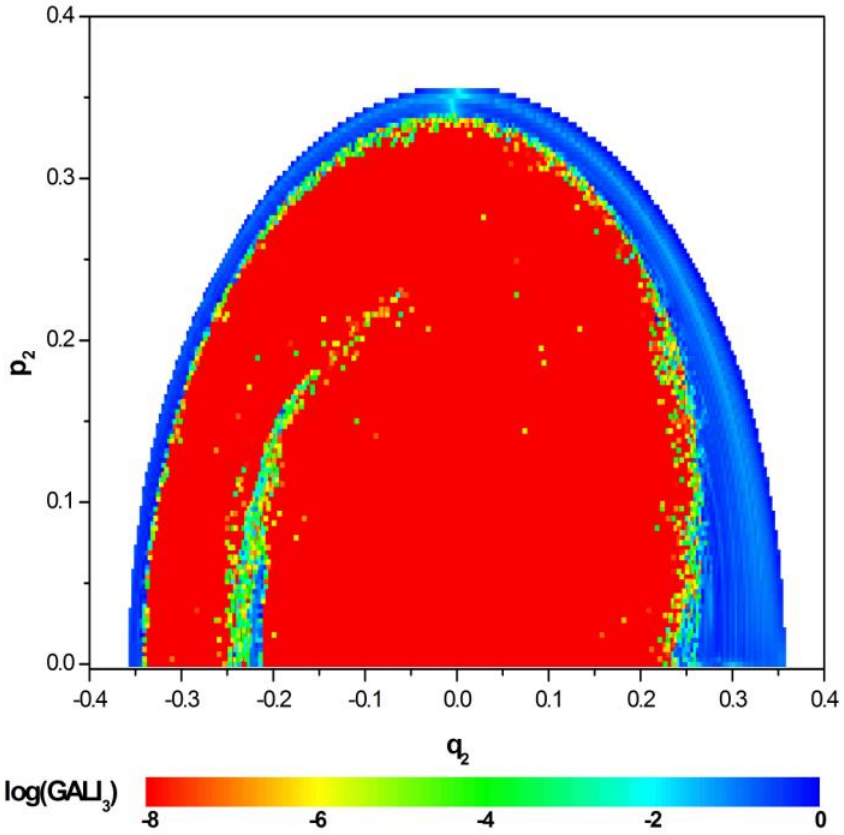

Global dynamics

$GALI_k$ with k>N

The index tends to zero both for regular and chaotic orbits but with completely different time rates:

Chaotic motion: exponential decay

Regular motion: power law

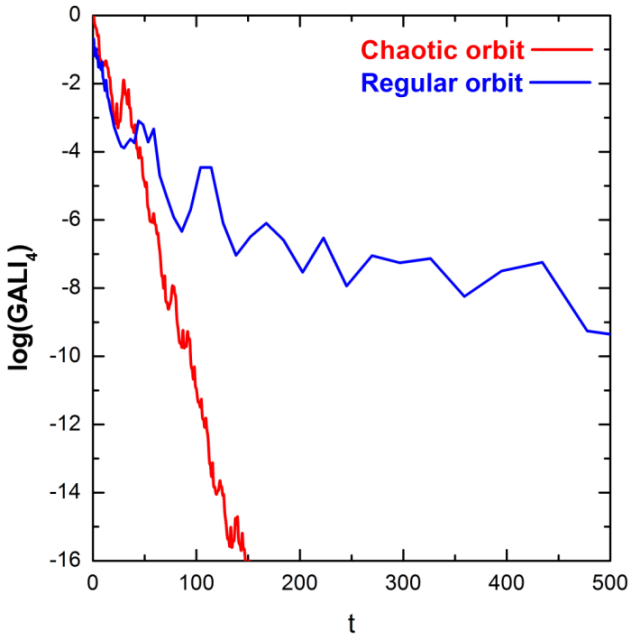

2D Hamiltonian (Hénon-Heiles)
Time needed for $GALI_4<10^{-12}$

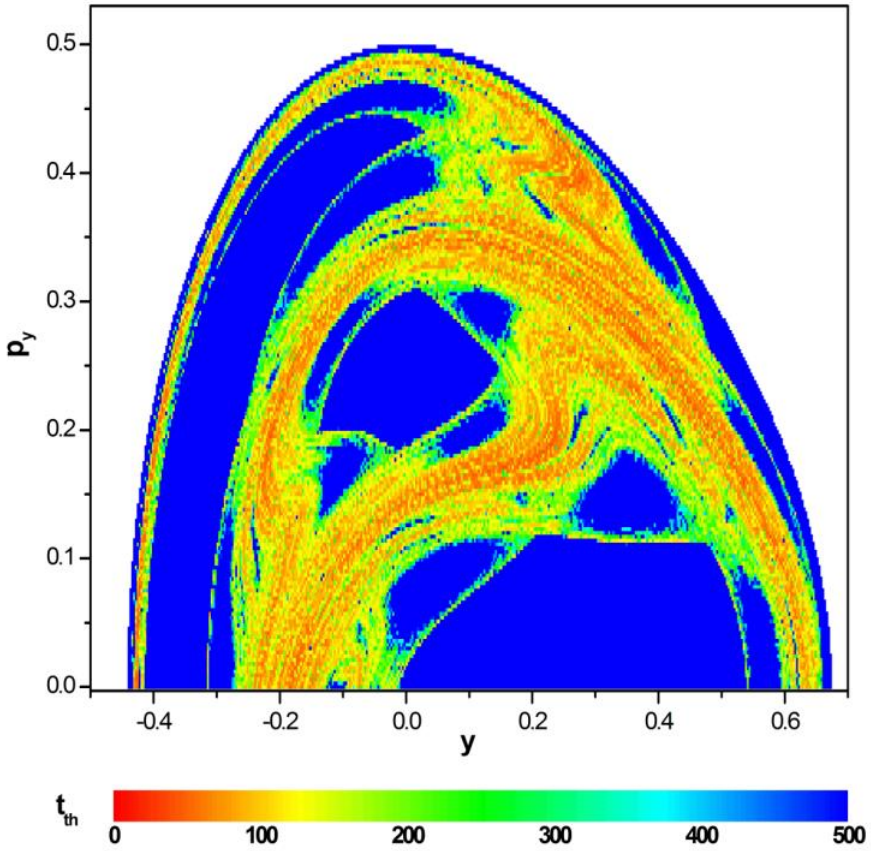

Behavior of $GALI_k$

Chaotic motion:

$GALI_k \to 0$ exponential decay

$$GALI_k(t) \propto e^{-[(\sigma_1-\sigma_2)+(\sigma_1-\sigma_3)+\ldots+(\sigma_1-\sigma_k)]t}$$

Regular motion:

$GALI_k \to$ constant $\neq 0$ or $GALI_k \to 0$ power law decay

$$GALI_k(t) \propto \begin{cases} \text{constant} & \text{if} \quad 2 \le k \le s \\ \dfrac{1}{t^{k-s}} & \text{if} \quad s < k \le 2N-s \\ \dfrac{1}{t^{2(k-N)}} & \text{if} \quad 2N-s < k \le 2N \end{cases}$$

Barred galaxies

NGC 1433

NGC 2217

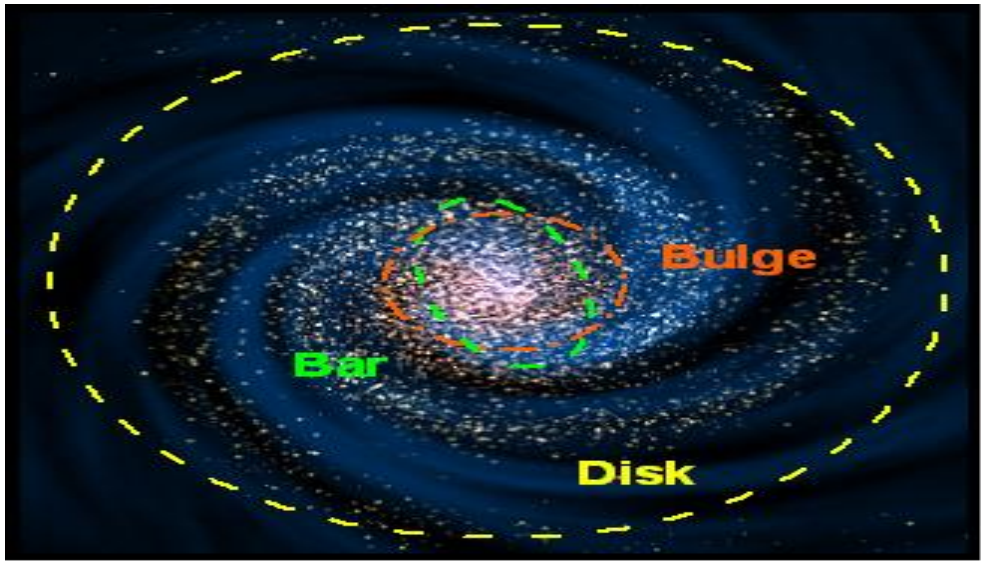

Barred galaxy model

The 3D bar rotates around its short *z*-axis (*x*: long axis and *y*: intermediate). The Hamiltonian that describes the motion for this model is:

$$H=\frac{1}{2}(p_x^2+p_y^2+p_z^2)+V(x,y,z)-\Omega_b(xp_y-yp_x)\equiv Energy$$

This model consists of the superposition of potentials describing an axisymmetric part and a bar component of the galaxy (Manos, Bountis, Ch.S., 2013, J. Phys. A).

a) Axisymmetric component:

i) Plummer sphere:

$$V_{sphere}(x,y,z)=-\frac{GM_S}{\sqrt{x^2+y^2+z^2+\varepsilon_s^{\,2}}}$$

ii) Miyamoto–Nagai disc:

$$V_{disc}(x,y,z)=-\frac{GM_D}{\sqrt{x^2+y^2+(A+\sqrt{B^2+z^2})^2}}$$

b) Bar component: $V_{bar}(x,y,z)=-\pi Gabc\frac{\rho_c}{n+1}\int_\lambda^\infty\frac{du}{\Delta(u)}(1-m^2(u))^{n+1},$

(Ferrers bar)

$$\rho_c=\frac{105}{32\pi}\frac{GM_B}{abc}$$

$$where\ m^2(u)=\frac{x^2}{a^2+u}+\frac{y^2}{b^2+u}+\frac{z^2}{c^2+u},\ \Delta^2(u)=(a^2+u)(b^2+u)(c^2+u),$$

n: positive integer ($n=2$ for our model), λ: the unique positive solution of $m^2(\lambda)=1$

Its density is:

$$\rho=\begin{cases}\rho_c(1-m^2)^n, & \text{for } m\le 1\\ 0, & \text{for } m>1\end{cases},\ \text{where } m^2=\frac{x^2}{a^2}+\frac{y^2}{b^2}+\frac{z^2}{c^2},\ a>b>c \text{ and } n=2.$$

Time-dependent barred galaxy model

The 3D bar rotates around its short *z*-axis (*x*: long axis and *y*: intermediate). The Hamiltonian that describes the motion for this model is:

$$H=\frac{1}{2}(p_x^2+p_y^2+p_z^2)+V(x,y,z,t)-\Omega_b(xp_y-yp_x)\equiv Energy$$

This model consists of the superposition of potentials describing an axisymmetric part and a bar component of the galaxy (Manos, Bountis, Ch.S., 2013, J. Phys. A).

a) Axisymmetric component:

$$M_S+M_B(t)+M_D(t)=1,\quad \text{with}\quad M_B(t)=M_B(0)+\alpha t$$

i) Plummer sphere:

$$V_{sphere}(x,y,z)=-\frac{GM_S}{\sqrt{x^2+y^2+z^2+\varepsilon_s^{\,2}}}$$

ii) Miyamoto–Nagai disc:

$$V_{disc}(x,y,z)=-\frac{GM_D(t)}{\sqrt{x^2+y^2+(A+\sqrt{B^2+z^2})^2}}$$

b) Bar component: $V_{bar}(x,y,z)=-\pi Gabc\frac{\rho_c}{n+1}\int_\lambda^\infty\frac{du}{\Delta(u)}(1-m^2(u))^{n+1},$

(Ferrers bar)

$$\rho_c=\frac{105}{32\pi}\frac{GM_B(t)}{abc}$$

$$where\ m^2(u)=\frac{x^2}{a^2+u}+\frac{y^2}{b^2+u}+\frac{z^2}{c^2+u},\ \Delta^2(u)=(a^2+u)(b^2+u)(c^2+u),$$

n: positive integer ($n=2$ for our model), λ: the unique positive solution of $m^2(\lambda)=1$

Its density is:

$$\rho=\begin{cases}\rho_c(1-m^2)^n, & \text{for } m\le 1\\ 0, & \text{for } m>1\end{cases},\ \text{where } m^2=\frac{x^2}{a^2}+\frac{y^2}{b^2}+\frac{z^2}{c^2},\ a>b>c \text{ and } n=2.$$

Time-dependent 2D barred galaxy model

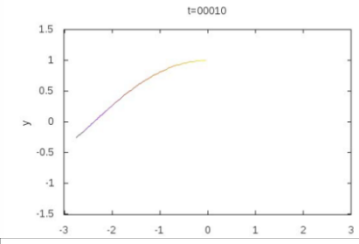

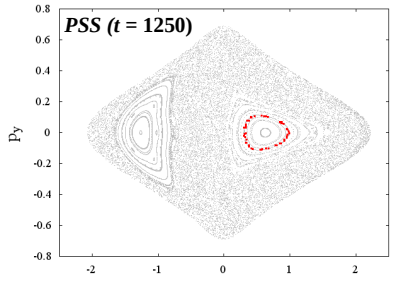

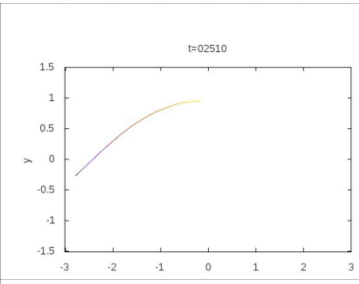

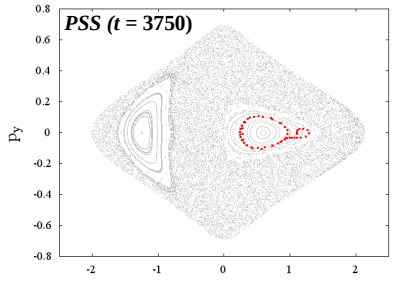

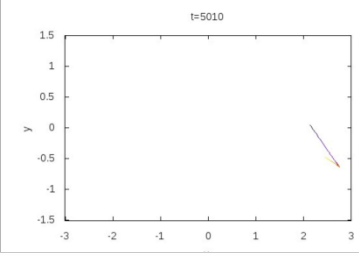

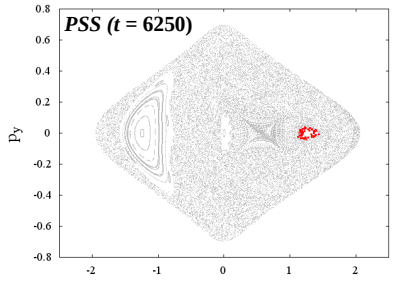

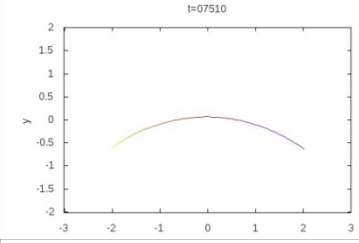

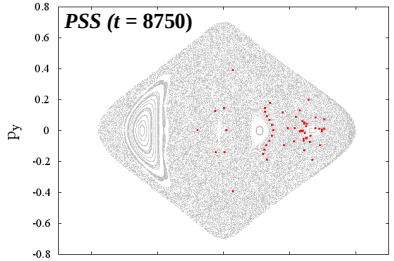

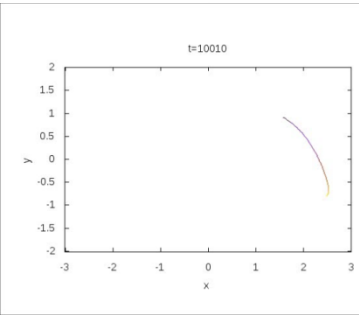

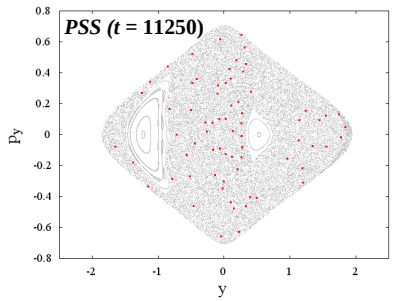

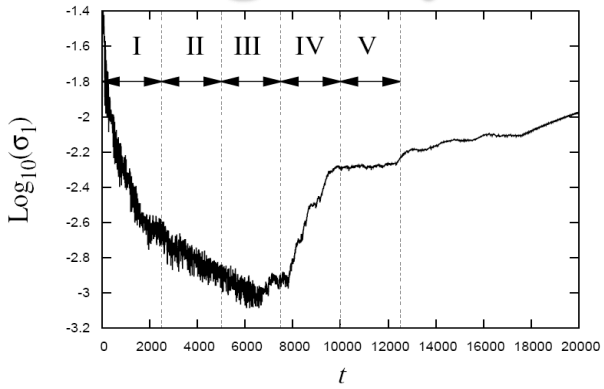

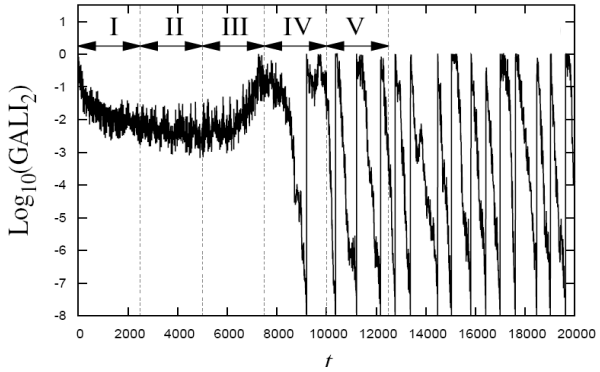

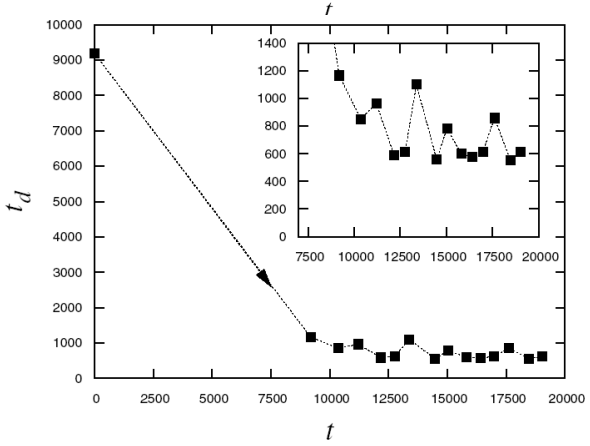

Time-dependent 3D barred galaxy model

Interplay between chaotic and regular motion

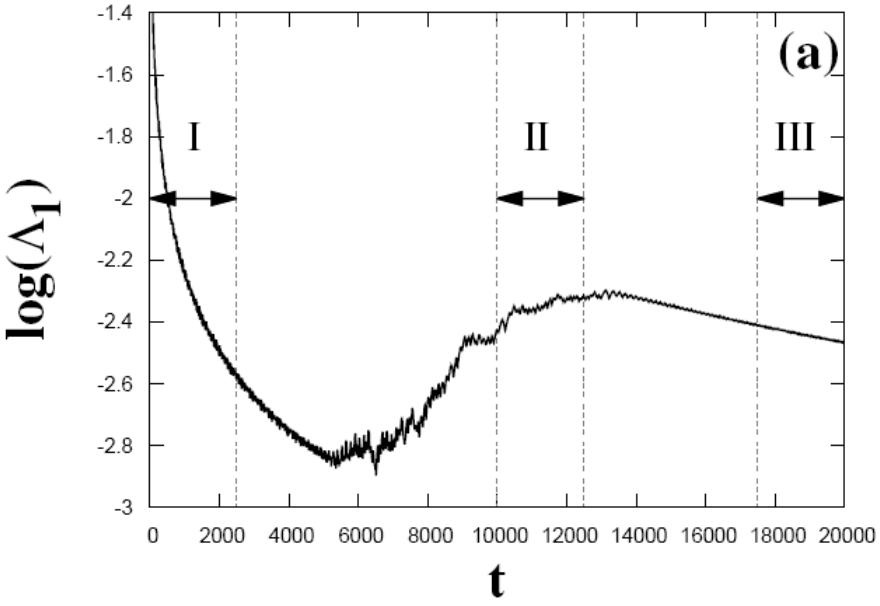

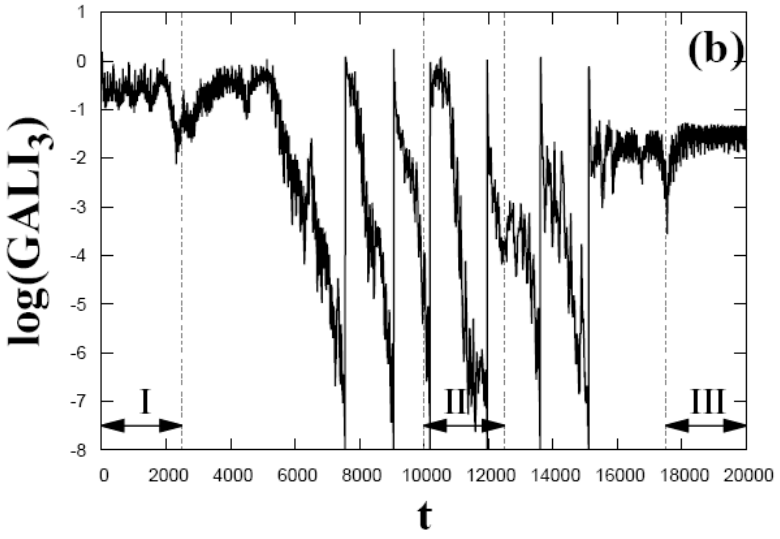

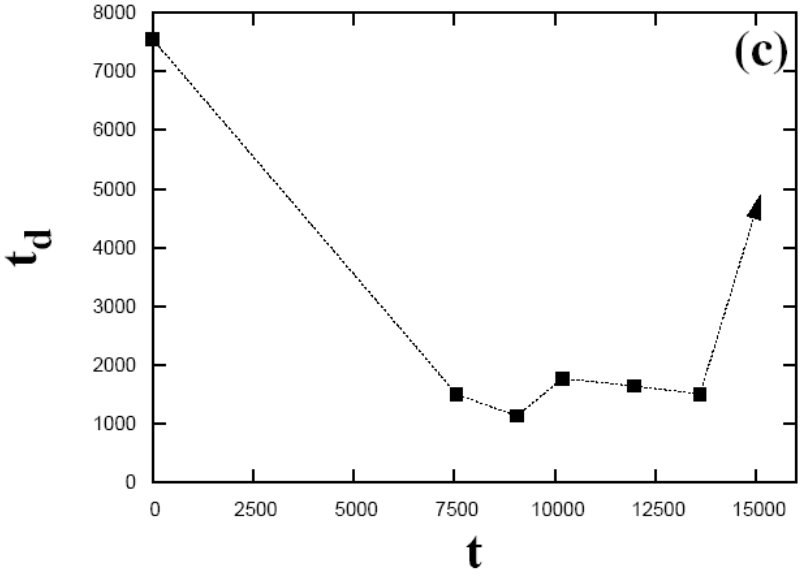

Conclusions I

- **The Smaller ALignment Index (SALI) method a fast, efficient and easy to compute chaos indicator.**

- **Behaviour of the SALI :**
  - ✓ **2D maps: it tends to zero following completely different time rates for regular and chaotic orbits, which allows the distinction between the two cases.**
  - ✓ **Hamiltonian flows and in multidimensional maps: it goes to zero for chaotic orbits, while it tends to a positive value for ordered orbits.**

Conclusions II

- **Generalizing the SALI method we define the Generalized ALignment Index of order k ($GALI_k$) as the volume of the parallelepiped, whose edges are k unit deviation vectors. $GALI_k$ is computed as the product of the singular values of a matrix (SVD algorithm).**

- **Behaviour of $GALI_k$:**
  - ✓ **Chaotic motion: it tends exponentially to zero with exponents that involve the values of several Lyapunov exponents.**
  - ✓ **Regular motion: it fluctuates around non-zero values for $2 \leq k \leq s$ and goes to zero for $s < k \leq 2N$ following power-laws, with s being the dimensionality of the torus.**

Conclusions III

- **$GALI_k$ indices :**
  - ✓ **can distinguish rapidly and with certainty between regular and chaotic motion**
  - ✓ **can be used to characterize individual orbits as well as "chart" chaotic and regular domains in phase space**
  - ✓ **are perfectly suited for studying the global dynamics of multidimentonal systems , as well as of time-dependent models**

- **SALI/GALI methods have been successfully applied to a variety of conservative dynamical systems of**
  - ✓ **Celestial Mechanics (e.g. Széll et al., 2004, MNRAS - Soulis et al., 2008, Cel. Mech. Dyn. Astr. - Voyatzis, 2008, Astron. J. - Libert et al., 2011, MNRAS - Racoveanu, 2014, Astron. Nachr.)**
  - ✓ **Galactic Dynamics (e.g. Capuzzo-Dolcetta et al., 2007, Astroph. J. - Carpintero, 2008, MNRAS - Manos & Athanassoula, 2011, MNRAS - Carpintero et al., 2014, MNRAS)**
  - ✓ **Nuclear Physics (e.g. Macek et al., 2007, Phys. Rev. C - Stránský et al., 2007, Phys. Atom. Nucl. - Stránský et al., 2009, Phys. Rev. E - Antonopoulos et al., 2010, PRE)**
  - ✓ **Statistical Physics (e.g. Paleari & Penati, 2008, Lect. Notes Phys. - Manos & Ruffo, 2011, Trans. Theory Stat. Phys. - Christodoulidi & Efthymiopoulos, 2013, Physica D)**

References

- **SALI**
  - ✓ Ch.S. (2001) J. Phys. A, 34, 10029
  - ✓ Ch.S., Antonopoulos Ch., Bountis T. C. & Vrahatis M. N. (2003) Prog. Theor. Phys. Supp., 150, 439
  - ✓ Ch.S., Antonopoulos Ch., Bountis T. C. & Vrahatis M. N. (2004) J. Phys. A, 37, 6269
  - ✓ Bountis T. & Ch.S. (2006) Nucl. Inst Meth. Phys Res. A, 561, 173
  - ✓ Boreaux J., Carletti T., Ch.S. &Vittot M. (2012) Com. Nonlin. Sci. Num. Sim., 17, 1725
  - ✓ Boreaux J., Carletti T., Ch.S., Papaphilippou Y. & Vittot M. (2012) Int. J. Bif. Chaos, 22, 1250219

- **GALI**
  - ✓ Ch.S., Bountis T. C. & Antonopoulos Ch. (2007) Physica D, 231, 30-54
  - ✓ Ch.S., Bountis T. C. & Antonopoulos Ch. (2008) Eur. Phys. J. Sp. Top., 165, 5-14
  - ✓ Gerlach E., Eggl S. & Ch.S. (2012) Int. J. Bif. Chaos, 22, 1250216
  - ✓ Manos T., Ch.S. & Antonopoulos Ch. (2012) Int. J. Bif. Chaos, 22, 1250218
  - ✓ Manos T., Bountis T. & Ch.S. (2013) J. Phys. A, 46, 254017

- **Reviews on SALI and GALI**
  - ✓ Bountis T.C. & Ch.S. (2012) 'Complex Hamiltonian Dynamics', Chapter 5, Springer Series in Synergetics
  - ✓ Ch.S. & Manos T. (2016), Lect. Notes Phys., 915, 129

A …shameless promotion

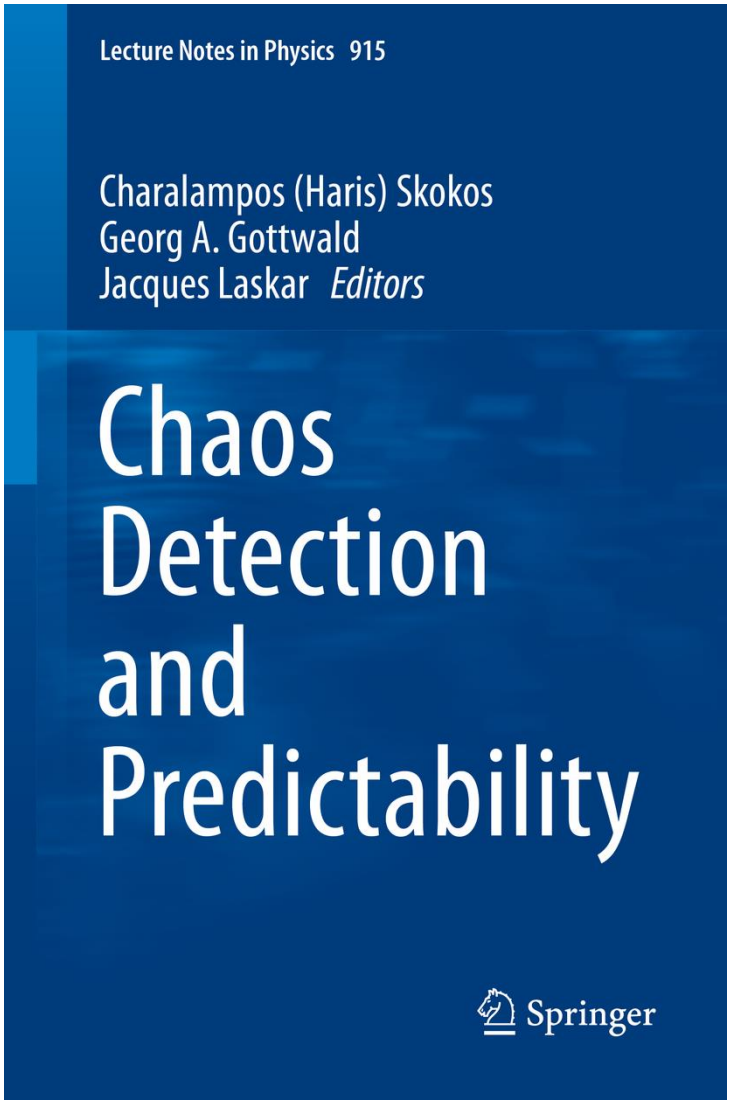

2016, Lect. Notes Phys., 915, Springer

Contents